Geologic map of the Mount Fagan 7.5' quadrangle, eastern Pima County, Arizona

by
Charles A. Ferguson, Ann Youberg, Wyatt G. Gilbert,
Tim R. Orr, Stephen M. Richard, and Jon E. Spencer

Arizona Geological Survey Digital Geologic Map 11 **v.2**

September, 2019

Scale 1:24,000 (1 sheet), with 34 page text

Arizona Geological Survey
416 W. Congress St., #100, Tucson, Arizona 85701

Research partially supported by the U.S. Geological Survey, National Cooperative Geologic Mapping Program, under USGS award number #00HQAG0149. The views and conclusions contained in this document are those of the authors and should not be interpreted as necessarily representing the official policies, either expressed or implied, of the U.S. Government.

INTRODUCTION

The Mount Fagan quadrangle is located approximately 30 km southeast of downtown Tucson, and includes the northern terminus of two mountain ranges; of the Santa Rita Mountains in the center and southwest, and the Empire Mountains along the eastern boundary. The northern portion of the quadrangle consists of a gently north-sloping piedmont surface carved into Quaternary basin-fill deposits in the northwest and rolling hills of bedrock in the northeast (Figure 1). The area was mapped during October, 2000 through May, 2001 as part of a multiyear mapping program directed at producing complete geologic map coverage for the Phoenix-Tucson metropolitan corridor. A 1:24,000 scale map is the primary product of this study (Plate 1). Mapping was done under the joint State-Federal STATEMAP program, as specified in the National Geologic Mapping Act of 1992, and was jointly funded by the Arizona Geological Survey and the U.S. Geological Survey under STATEMAP Program Contract #00HQAG0149.

Bedrock geology of the Mount Fagan quadrangle is exceptionally complex. To complicate matters, exposure is poor in many areas and access to large areas of the northern Santa Rita Mountains is difficult, owing to a myriad of small private land holdings. Consequently, a large portion of our map in the northern foothills of the Santa Rita Mountains is taken directly from a preliminary geologic map of the area by Finnell (1971; Plate 1). Since the reproduction of Finnell's (1971) map is quite poor, many of the contacts in the area of his mapping are not well located, and some of the unit designations are uncertain. For these reason and others, the geologic map of the Mount Fagan must be considered a work in progress. Future study of several exceptionally complex areas could be illuminating. Interested readers should be aware that updates of the digital map coverage could be released in the future.

Surficial geologic mapping of the Mount Fagan quadrangle builds on and complements previous surficial geologic mapping efforts in the Tucson area (McKittrick, 1988; Jackson, 1989, 1990; Demsey and others, 1993; Klawon and others, 1999; Pearthree and Biggs, 1999, Pearthree and Youberg, 2000). This report is intended to enhance our understanding of the surficial geology of the area and to aid in assessing and understanding geologic hazards.

ACKNOWLEDGMENTS

We thank Bill McIntosh and Lisa Peters for providing two $^{40}Ar/^{39}Ar$ dates of an important welded ignimbrite at the base of the Tertiary sequence. Many landowners in the area graciously allowed access to private lands in the foothills of both mountain ranges, and provided succor on many hot afternoons. In particular we thank Don and Glenda Martin, Ted and Sandra Notz, Joe Patterson and Kathleen McNaboe, George and Erin Grinnan, Spencer Brown, Karen Wilsey and Leslie Cook, Tom Spencer, Roger Helm, Russell Stewart, Doug Alewelt, and Dave Tenpenney. We also thank the US Forest Service and Jim Briscoe of JABA LLC for providing aerial photographs of the map area. We especially thank Philip Pearthree for field support, guidance and discussions that were helpful in understanding the Santa Rita fault, and Ramon Arrowsmith for providing access to his model for estimating morphological ages of scarps.

Charles Ferguson would like to dedicate this work to the memory of David Charles Decker, 1949-2001.

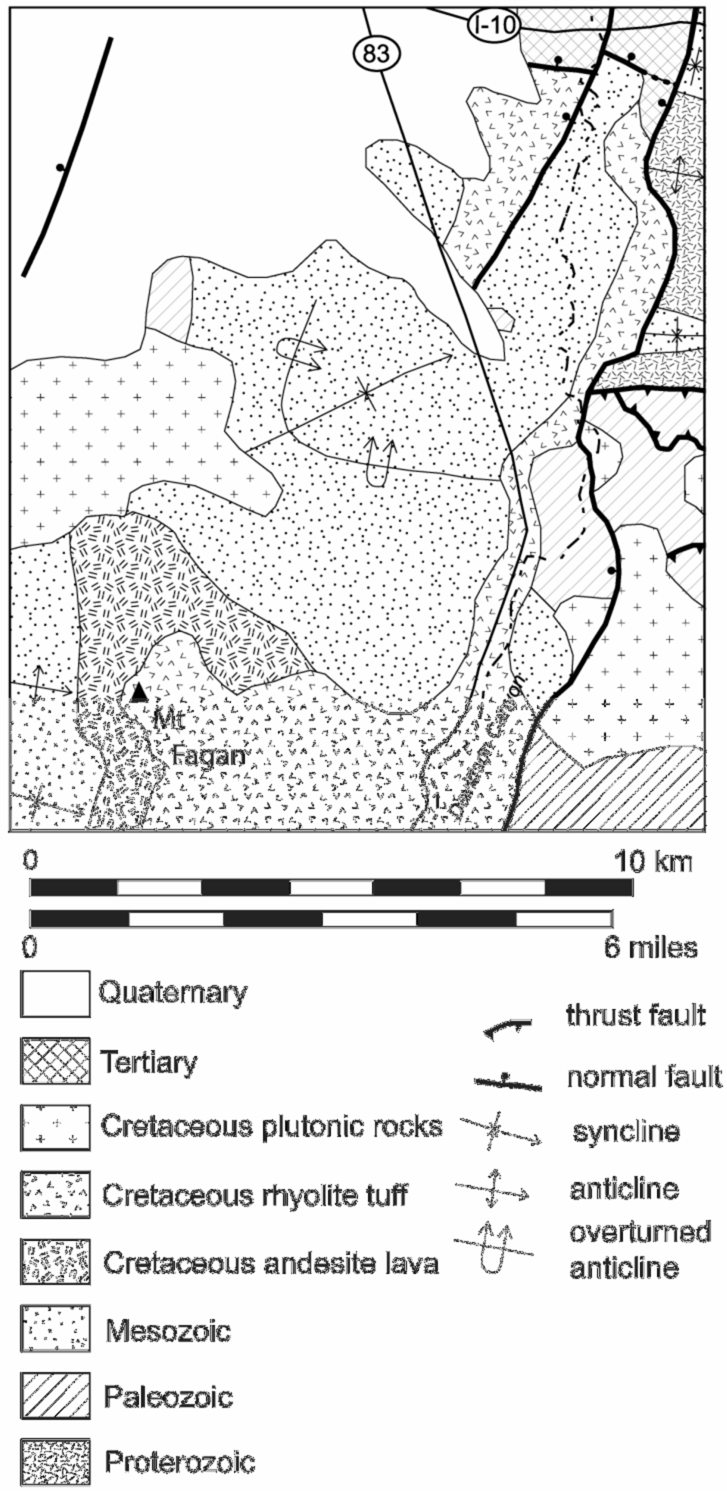

Figure 1. Simplified geology of the Mount Fagan 7.5' quadrangle.

SUMMARY OF IMPORTANT FEATURES, PROBLEMS, AND SUGGESTIONS FOR FUTURE WORK

The bedrock geology of the map area is dominated by seven sets of rock units, each bounded by significant unconformities. Crystalline basement (1) is composed of mica schist intruded by an extensive pluton of equigranular granodiorite of probable Early Proterozoic age, and lesser amounts of younger, probably Middle Proterozoic, porphyritic, coarse-grained granite. Paleozoic and carbonate and siliciclastic rocks (2) disconformably overlie the crystalline basement in the south, but are conspicuously absent to the north, where siliciclastic rocks of the Jurassic-Cretaceous Bisbee Group (4) directly overlie the Proterozoic rocks. A thin sequence of early to middle Mesozoic volcaniclastic red beds intercalated with sparse volcanic rocks (3) is present locally in the south, but its upper and lower contact relationships are typically disrupted by low-angle faults. In some areas, the red beds merge imperceptibly upwards into conglomeratic rocks of the basal Bisbee Group. In the area where the Paleozoic section is abruptly omitted from the section at the north end of the Empire Mountains the Glance Conglomerate, a thick succession of coarse-grained conglomerate which thins rapidly to the south, marks the base of the Bisbee Group. This wedge of coarse-grained debris overlaps a south-facing paleoescarpment related to formation of the latest Jurassic Bisbee trough. At least two phases of Laramide folding affect the Bisbee Group. In the Santa Rita Mountains the Bisbee Group is overlapped, along a pronounced angular unconformity, by a conformable and apparently continuous succession of Upper Cretaceous nonvolcaniclastic conglomerate (Fort Crittenden Formation) overlain by a pile of subaqueous mafic-intermediate lava, and a silicic ash-flow tuff of the Salero Formation (5). All of these rocks are intruded by Upper Cretaceous granodiorite stocks, and a suite of northwest-striking quartz porphyry dikes and related stocks (6). Fanglomerate, minor mudstone, limestone, and lava flows of the mid-Tertiary Pantano Formation occur in the northeast (7). Quaternary deposits are locally deeply incised along principle drainages in the northern part of the quadrangle, and in the northwest they are cut by a NNE-striking, west-side-down normal fault that represents youthful activity along the western range bounding fault system of the Santa Rita Mountains.

Several important regional tectonic and stratigraphic elements converge in the Mount Fagan area and one of the most significant new findings of our work concerns the mid-Jurassic Bisbee trough. The Bisbee trough is a complex, generally east-west trending basin which extends into the study area from the southeast (Bilodeau et al., 1987; Dickinson et al., 1987, 1989). Dramatic syndepositional thickening of the Bisbee Group is represented in the Mount Fagan quadrangle by a sequence of siliciclastic sedimentary rocks that thicken abruptly to the south of a south-facing paleoescarpment. The escarpment is overlapped to the south by up to 1500 meters of Glance Conglomerate, the basal unit of the Bisbee Group. To the north however, only a thin ($\leq$ 50 meter thick) sequence of Glance Conglomerate is overlain by strata of the Turney Ranch lithofacies, the youngest unit of the Bisbee Group in the area. Nearly 2,000 meters of middle Bisbee Group strata, well represented to the south, are missing to the north of the escarpment. In addition, to the north of the escarpment, Bisbee Group directly overlies Proterozoic basement, whereas to the south the Bisbee Group overlies a section of Paleozoic rocks estimated (Finnell, 1971) to be nearly 2,000 meters thick. The intervening escarpment therefore represents approximately 4 kilometers of south-side-down offset. The escarpment has been interpreted as a south-side-down normal fault or fault zone that was later cut by north-dipping, south-vergent, Laramide thrust faults Bilodeau (1979) and Bilodeau et al. (1987). We believe, however, that the Laramide thrust(s) are south-dipping and north-vergent, and that they reactivated the older south-side-down normal fault(s).

Another significant new finding of our mapping is that the Bisbee Group was folded twice. The best evidence for multiple deformation is in the northwest corner of the easterly adjacent Narrows quadrangle, where a tight to isoclinal synclinal keel of Bisbee Group is folded about a broad, open, east-plunging antiform (Spencer et al., 2001). In the central Mount Fagan quadrangle, a large area of Bisbee

Group mapped by Finnell (1971), is interpreted as a regional, tight to isoclinal anticline that is folded about a broad, open, east-plunging synform.

The southwestern corner of the Mount Fagan quadrangle is transected by a deep trough, at least 3 kilometers deep, of Upper Cretaceous volcanic rocks of the Salero Formation. As documented by Finell (1970; 1971) the Salero Formation and a basal conglomerate unit (Fort Crittenden Formation) overlie the folded Bisbee Group with pronounced angular unconformity. The trough-filling volcanic rocks overlap the inferred up-thrown side of an inferred, southwest-side-down, northwest-striking fault zone. The trough is filled by at least 1 kilometer of subaqueaous andesitic lava, and above this 1-2 kilometers of silicic, caldera-filling ignimbrite with enormous blocks and extensive swarms of lithic debris. The ignimbrite, herein named the rhyolite of Mount Fagan overlaps the northeast margin of the trough (the andesitic lavas are confined within) and extends as an intracauldron unit at least 12 kilometers to the northeast. Throughout the map area, the rhyolite of Mount Fagan contains abundant megabreccia blocks and swarms of mesobreccia. This implies that all pre-Salero Formation rocks in the northern foothills of the Santa Rita Mountains were at one time below the floor of a major caldera.

The Santa Rita and Empire mountains are separated by a major, west-side-down fault zone. In the northeast corner of the map area two major west-side-down faults with a combined offset of at least 3,000 meters cut the mid-Tertiary Pantano Formation. The western fault can be traced south-southwest for several kilometers across the peidmont, but from here it is buried by piedmont deposits and it is not clear where it extends to the south. The eastern fault was traced across the sporadically exposed northern pediment of the Empire Mountains by assuming that all exposures of the rhyolite of Mount Fagan are in its hanging wall. This approach produces a somewhat irregular map pattern. Farther south, the fault is assumed to coincide with an important west-side-down fault that cuts through the Empire Mountains stock along the west flank of the range. Finnell (1971) interpreted this fault to be intruded by the stock, but we found that, although some strands appear to be intruded by the stock, a main strand clearly cuts the stock. We interpret the younger strand(s) of the fault zone to be related to motion on the Davidson Canyon fault zone, and the intruded fault strands to be related to syn-volcanic tectonism associated with emplacement of the rhyolite of Mount Fagan. The intruded fault strands may be part of a west-facing cauldron margin, and if so the margin may have influenced the location of the Davidson Canyon fault.

Due to the complexity, poor exposure, and difficult access of many key areas in the Mount Fagan quadrangle, we stress that this map is, even more than others, a work in progress. We intend to continue examining some of these key areas in the near future, but in the event that we are unable to revisit the map area we suggest three key areas for continued work.

1) The large area of folded Bisbee Group intruded by extensive dikes and stocks of the quartz porphyry map unit (Tq) in the center of the map needs to be studied in more detail. Confirming or dismissing our interpretation of this area as a refolded fold is of critical importance.

2) The low-angle faults along Davidson Canyon and around Davidson Spring are poorly understood. Although the map patterns are fairly well demarcated, the origin of these important structures is somewhat cryptic. The faults may be related to at least three separate events, Laramide compressional deformation, Late Cretaceous caldera formation, and Mid-Tertiary extension, or they could have been reactivated several times. Detailed studies of the fault surfaces may reveal some important clues.

3) A complex, northwest-striking, southwest-side-down fault zone in the southeast corner was mapped by Finnell (1971), but not examined by us. It seems likely that this is a deep expression of the major, synvolcanic structure in the Santa Rita Mountains, but thrust slivers along the fault mapped by Finnell (1971) suggest that the fault may have, among other things, a strike-slip component.

QUATERNARY

Climate

Several weather stations located near the map area that have operated during intervals over the past century provide climatological data for the study area. The current Tucson Weather Service Office at Tucson International Airport (WSO, about 10 miles west of the map area) has records from 1948 to the present and the weather station maintained at the Santa Rita Experimental Range Headquarters (ERH, about 10 miles southwest of the map area) has records from 1950 to present. Stations were maintained at Benson (about 20 miles east of the map area) from 1894 to 1975, and at Helvetia (just west of the map area) from 1916 to 1950. Throughout this region, most of the annual precipitation (50-60%) falls during the summer monsoon from June to September. Late summer rainfall occurs as heavy thunderstorms when moist air sweeps northwards from the Gulf of California and the Gulf of Mexico. Occasional intense late summer to early fall precipitation occurs in this region as a result of incursions of moist air derived from dissipating tropical storms in the Pacific Ocean. Winter precipitation generally is caused by cyclonic storms originating in the Pacific. It is usually less intense and may be more prolonged, and therefore infiltrates into the soil more deeply than summer rainfall (summarized from Sellers and Hill, 1974). Freezing temperatures are common during most winters, but snow is uncommon and not persistent.

Climate records from the WSO, at about 2500 ft asl, and Benson, at about 3500, show similar average annual precipitation and temperatures for slightly different time periods. Average annual precipitation is 11.6 in. for the WSO, and 11.3 in. for Benson (Western Regional Climate Center, 2001). The average maximum temperature for the WSO is 82.5° F, with an average high temperature of 99.1° F in July and 64.7° F in January. Benson is slightly cooler. ERH and Helvetia, both near 4300 ft asl, may provide a better representation of precipitation and temperature patterns for the map area as it is generally higher than either the WSO or Benson. Average annual precipitation for the ERH and Helvetia are 22.3 and 19.7 inches, respectively, which is nearly double the average annual precipitation for the WSO or Benson. The average maximum temperature at the ERH is 76.4° F, with average high temperatures of 91.6° F in July and 60.2° F in January. The average maximum temperature at Helvetia is 75.6° F, with average high temperatures of 91.3° F in July and 57.9° F in January. The average annual precipitation for ERH is probably a maximum for the map area because of its proximity to the base of the Santa Rita Mountains.

Methodology

The surficial geology of the project area was mapped using color 1:48000 aerial photographs taken in 1979, provided by James Briscoe of JABA LLC, and color aerial photos taken in 1987, provided by the US Forest Service. Unit boundaries were checked in the field, and mapping was supplemented by observations and descriptions of soils and stratigraphy. The physical characteristics of Quaternary alluvial surfaces (channels, alluvial fans, floodplains, stream terraces) evident on aerial photographs and in the field were used to differentiate their associated deposits by age. Surficial deposits of this quadrangle were then correlated with similar deposits in this region in order to roughly estimate their ages. Original mapping was done on aerial photos and compiled on a 7 ½' quadrangle map. The map compilation was then digitized and the final map was generated from the digital data.

The physical characteristics of Quaternary alluvial surfaces (channels, alluvial fans, floodplains, stream terraces) were used to differentiate their associated deposits by age. Alluvial surfaces of similar age have a distinctive appearance and soil characteristics because they have undergone similar post-depositional modifications. They are different from both younger and older surfaces. Terraces and alluvial fans that are less than a few thousand years old still retain clear evidence of the original depositional topography, such as bars of gravel deposits, swales (troughlike depressions) where low flows passed between bars, and distributary channel networks, which are characteristic of active alluvial fans. Young alluvial surfaces have little rock varnish on surface clasts and have little soil development, and they are minimally dissected. Very old fan surfaces, in contrast, have been isolated from substantial fluvial deposition or reworking for hundreds of thousands of years. These surfaces are characterized by strongly developed soils with clay-rich argillic horizons and cemented calcium-carbonate horizons, well-developed tributary stream networks that are entrenched 1 to 10 m below the fan surface, and strongly developed varnish on surface rocks. The ages of alluvial surfaces in the southwestern United States may be roughly estimated based on these surface characteristics, especially soil development (Gile and others, 1981; Bull, 1991).

In this map, Quaternary surficial deposits are subdivided based on their source (axial valley streams and smaller tributary washes on piedmonts) and estimated age of deposits. Surface and soil characteristics were used to correlate alluvial deposits and to estimate their ages. Surface pits and exposures along cut banks were used to assess soil characteristics associated with deposits of different ages and from different sources. Soils and surfaces documented in the map area were generally correlated with soils and surfaces described in Quaternary mapping studies of adjacent areas conducted by Katzer and Schuster (1984), McKittrick (1988), Jackson (1989, 1990), Demsey and others (1993), Klawon and others (1999), Pearthree and Biggs (1999), and Pearthree and Youberg (2000). These correlations were also used to estimate the ages of surficial deposits in the map area.

Geologic/Geomorphic Framework

The Mount Fagan quadrangle is located southeast of the Tucson Metropolitan area along the eastern edge of the Sonoran Desert subprovince of the Basin and Range physiographic province. The Basin and Range province in Arizona is characterized by alluvial basins and intervening mountain ranges that formed as a result of normal faulting related to extension of the crust between about 30 and 6 Ma (Shafiqullah and others, 1980; Menges and Pearthree, 1989). The landscape of the Tucson area consists of alluvial basins between large, high mountain ranges to the east and small, low-lying mountain ranges to the west. The western part of the metropolitan area (Avra Valley and the west side of the Tucson Mountains) is typical of the undissected basins that are common throughout the Sonoran Desert subprovince. Mountain ranges are low and mountain fronts are deeply embayed, with few outlying bedrock knobs (inselbergs) that rise above the broad plains surrounding the mountain ranges. Upper piedmont areas typically are covered with Pleistocene deposits that are moderately dissected, but lower piedmont areas are undissected and covered by relatively fine-grained young deposits that grade downslope into axial valley deposits. The axial portions of valleys are typically occupied by unentrenched drainages with very broad floodplains. In stark contrast, the eastern, northern, and southern parts of the Tucson area have large, high mountain ranges and piedmont areas have been deeply dissected by erosion. In these areas, erosion has dominated landscape evolution at least through the Quaternary. Major periods of aggradation have punctuated the long-term trend toward downcutting along the major streams and their tributaries, resulting in the formation of terraces along these watercourses.

The highest levels of alluvial deposits (unit QTs ridgelines and Qo surfaces, found on the extreme western edge of the map area) may have been graded approximately to the Tucson basin before it was significantly entrenched. They are probably approximately correlative with QT deposits mapped in the Catalina foothills on the north side of the Tucson basin (Klawon and others, 1999), Qo and QT deposits mapped in the Tucson Mountain foothills on the west side of the Tucson basin (Pearthree and Biggs, 1999), and other high remnant deposits throughout southeastern Arizona (Menges and McFadden, 1981). It is likely that in the late Pliocene to early Quaternary, these alluvial surfaces were fairly planar, undissected piedmonts that graded downslope to a large alluvial fan complex that emanates from the Davidson Canyon area westward across the Tucson basin.

Erosion has dominated landscape evolution at least through the Quaternary. Major periods of aggradation have punctuated the long-term trend toward downcutting along the major streams and their tributaries. During the past one to two million years, Cienega Creek and its tributaries have downcut substantially into the Quaternary and Tertiary deposits of the map area. The high ridges and deep valleys characteristic of parts of the piedmont attest to the amount of stream erosion that has occurred since the highest levels of alluvium were deposited. Episodes of downcutting of Cienega Creek caused erosion of the toes of alluvial fans on both sides of the valley, and resulted in much of the stream downcutting in the piedmonts adjacent to the creek. Streams that head in the Santa Rita and Empire mountains flow across the piedmonts and eventually join Cienega Creek. The lower ends of these streams are linked with the creek, so episodes of downcutting in Cienega Creek tends to steepen and downcut the slopes of its tributary stream channels as well. The ultimate cause of the downcutting by the larger streams in southeastern Arizona is not certain. It is may have occurred a delayed response of the integration of the Tucson basin streams into the larger regional drainage system. The oscillating climatic conditions of the Quaternary may have resulted in higher long-term erosion rates than during the Miocene and Pliocene (Peizhen and others, 2000). Alternatively, the downcutting may have been driven by some broad regional upwarping of southeastern Arizona, the cause of which is not known (Menges and Pearthree, 1989).

The fact that we observe suites of alluvial surfaces with similar characteristics and topographic relationships throughout southern Arizona implies that the factors that are controlling erosion and deposition in fluvial systems are regional in scope. Whether fluvial systems aggrade or degrade is a function of sediment supply and their ability to transport sediment. Most of the area within drainage systems consists of hillslopes, where sediment is generated from weathering of bedrock and in turn is weathered in place and/or transported downslope to the stream system. If hillslopes are stable, then weathering dominates and sediment supply to streams is relatively low. These conditions probably existed in this region during glacial intervals, when vegetation density on hillslopes was greater due to increased annual precipitation and/or decreased summer temperatures in this region. Hillslopes have probably been unstable during changes between glacial and interglacial conditions, as vegetation responded to changing climate and the character of precipitation and runoff varied in response to changes in the nature and frequency of thunderstorm activity. As a result of these climate-induced changes, large fluxes of sediment may have been introduced into the fluvial systems, causing periods of aggradation on the piedmont. The fans and terraces of the map area likely record climate changes of this kind.

Geologic Hazards

This section summarizes the character and distribution of the principal geologic hazards that exist in and around the map area. This information is fairly general in nature. Detailed site-specific geologic, engineering, hydrologic, or soils investigations may be required to thoroughly assess potential hazards at particular locations. More specific information on soil properties may be obtained from the USDA Natural Resources Conservation Service, and information on mapped floodplain and flood-prone areas may be obtained from the Pima County Flood Control District.

Flood hazards

Hazards related to flooding in the map area may be subdivided into two broad categories. Along Davidson Creek and its tributaries, flood hazards consist mainly of channel and floodplain inundation and lateral erosion of unprotected channel banks. The most widespread flood hazards are those associated with smaller tributary drainages on piedmonts, where the extent of flood-prone area varies with the size of the stream and local topographic confinement of floodwater. This latter category of flood hazard is particularly difficult to assess in areas where channel networks are distributary and topographic relief is low. These areas may be subject to alluvial fan flooding.

The largest floods on Cienega and Davidson creeks have occurred in the middle to late summer or early fall (July through October). A USGS stream gage measured flow on Davidson Canyon 0.3 miles upstream from I-10 from 1968 to 1982. The largest recorded flow, 6,860 cfs, was in July of 1970. Long-term stream gages that are useful for the study area are located on Pantano Wash, north of the map area. The name Pantano Wash is used for the stream below the confluence of Cienega and Agua Verde creeks, so it is part of the same drainage as Cienega Creek and Davidson Creek. The closest gage (Pantano Wash near Vail) is just north of the map area. Moderate to large floods on Pantano Wash occurred in 1941, 1958, 1959, 1963, 1964, 1981,and 1983. At the Pantano gage near Vail, the 38,000 cubic feet per second (cfs) discharge in August, 1958 is the peak of record (Pope and others, 1998; U.S. Geological Survey, 2001). In fact, the estimated peak discharge for this flood is 3 times larger than any other flood of the gage record. Prior to the gage record, large summer floods on Cienega Creek in the 1880's and 1891 began the development of the modern entrenched arroyo system (Myrick, 1975). All of the sizable floods on Pantano Wash have occurred in August, September, or early October. This suggests that exceptional summer monsoon storms and occasional dissipating tropical storms generate the floods on this small regional drainage.

Smaller tributaries that drain the mountain ranges and the piedmonts are subject to flash floods. Floods on these drainages result from intense, localized thunderstorms that occur during the summer or early autumn, and stream stages typically rise and fall rapidly during floods. Flood hazards are relatively easy to manage where topographic relief contains floodwater to channels and adjacent low terraces. In these situations, the area that may be impacted by flooding is limited and should be easy to avoid. It is much more difficult to assess and manage flood hazards associated with alluvial fan flooding. This type of flooding occurs where topographic relief is minimal and floodwater can spread widely. In these areas, channels may or may not be well defined, their positions may shift during floods, and inundation is likely to be widespread during floods.

Surficial geologic mapping provides important information about the extent of flood-prone areas on the piedmonts, and it is the best way to delineate areas that may be prone to alluvial fan flooding. Floods leave behind physical evidence of their occurrence in the form of deposits. Therefore, the extent of young deposits on piedmonts is a good indicator of areas that have been flooded in the past few thousand years. These are the areas that are most likely to experience flooding in the future. Following this logic, the extent of potentially flood-prone areas on the piedmont varies with the extent of young deposits (units Qy_2, Qy_1, and Qy). Active alluvial fans may be recognized by both distributary (downstream-branching) channel networks and laterally extensive young deposits between channels (see Pearthree and others, 1992).

Most of the modern drainages on the piedmonts have tributary networks that are topographically confined by ridges of older alluvium. Along these drainages, flood hazards are restricted to active channels and adjacent low, young terraces (unit Qy_2 or Qy). Portions of the slightly older and higher terraces that are mapped as unit Qy_1 may be subject to rare inundation in extreme floods. There are a some distributary drainage systems on the lower piedmont areas, especially in the northwestern portion of the map area, that are subject to broad sheetflooding and possibly alluvial-fan flooding. Flood hazards are greatest at the upslope end of these areas, at the transition from confined to unconfined flow, because of fairly deep flow, high flow velocities, and the potential for significant changes in channel position during floods. Unconfined flow during floods occurs along floodplain margins of Davidson Creek, where tributaries debouch from the topographically confined foothills onto the Qy_{1r} terraces.

Soil problems

Soils in the Tucson area present a number of problems to homeowners. Cracking of foundations, walls, driveways and swimming pools causes headaches and costs millions of dollars each year in repairs. Severe or recurring damage can lower the value of a house or commercial property. Leading in the list of potential soil properties that can cause structural failures are expansive soils and collapsing soils. Properties of problem soils are generally related to the type and amount of clay, and to the conditions under which the clay originated. Clay minerals can form in-place by weathering of rocks, or by deposition from water or wind.

Potential soil problems in middle and upper piedmont areas consist of shrink-swell potential, low infiltration rates, and hard substrate. Shrink-swell problems may exist on clay-rich soils of unit Qm, Qmo, and Qo, although the gravel that is common in these deposits may minimize these problems. Excavation may be difficult and near-surface infiltration rates low on the oldest piedmont units (Qmo, Qo, and QTs) due to the existence of carbonate- and silica-cemented hardpans (petrocalcic and duric horizons). Excavation and infiltration problems may be encountered on all surficial units in the uppermost piedmont areas because of the existence of bedrock at shallow depths.

Land subsidence and earth fissures

In the Tucson area, agricultural development and population increases have resulted in the heavy use of groundwater resources. Because groundwater recharge in the area is limited, groundwater levels have been lowered up to several hundred feet in parts of the Tucson area. Earth fissures have developed in Avra Valley, and recent measurements have indicated that the surface of the central part of the Tucson basin (northeast of the map area) has begun to subside.

Withdrawal of groundwater at rates faster than natural recharge leads to declines in water tables. Water levels in parts of Tucson’s central well field had declined by more than 150 feet by 1981 (Anderson, 1988) and are continuing to decline. Water levels have declined by 50 to 150 ft in most of Avra Valley, but levels may not be declining in that area at present (Anderson, 1989). Dewatering of sediments causes compaction, which in turn results in lowering of the land surface. In every Arizona groundwater basin where groundwater overdraft has occurred, subsidence has followed. Land subsidence is as much as 15.4 feet near Eloy (Slaff, 1993) and 18 feet west of Phoenix (Schumann, 1992). In the Tucson basin, subsidence was detected in re-leveling surveys in 1952 (Platt, 1963), but maximum total subsidence was only about 0.5 feet by 1980 (Anderson, 1988).

Recent surveys have indicated continuing subsidence as water levels decline under Tucson. Hatch (1991) measured an average subsidence rate of 1 cm per year over the Tucson basin from 1987 to 1991. Based on the amount and rate of past subsidence, parts of the Tucson basin can expect subsidence of more than 10 feet by the year 2030 (Anderson, 1988). In Avra Valley, 10 ft or more of subsidence is possible in the northern part of the basin if water levels continue to decline (Anderson, 1989). Measurements in the Tucson basin suggest that the rate of subsidence has increased markedly since 1980. Confirmation of the increased rate of subsidence is provided by a preliminary survey of subsidence using satellite-based synthetic aperture radar interferometry. Using SAR interferometry, a British company measured 9 cm of subsidence over a 3 year, 9 month period, ending in March, 1997, yielding a rate of 2.4 cm/yr (Galloway and others, 1999).

In Arizona basins where subsidence is more than a few feet, earth fissures have developed. A fissure developed in northern Avra Valley east of Marana High School adjacent to the Central Arizona Project aqueduct (Arizona Geological Survey, 1988). It was quickly filled and surface water was diverted from it, and it has not reopened. The Tucson basin is the only one of Arizona’s deep groundwater basins where groundwater level declines and land subsidence have not yet been followed by earth fissures, probably because the amount of total subsidence has thus far been relatively small compared to other basins. With the expected lowering of water tables and subsequent predicted land subsidence, earth fissures may be expected to develop in Tucson as they have elsewhere.

Earthquake hazards

There has been very little historical seismic activity in southeastern Arizona with the exception of the Sonoran earthquake on May 3, 1887. This magnitude ~7 ¼ event, centered southeast of Douglas, Arizona, caused strong shaking and damage throughout southeastern Arizona. Later that year, at least two earthquakes were reported from observers on the railroad in the Pantano area (DuBois and others, 1982). Based on the location of the maximum shaking reported for these events, they were likely located just east of the map area, in or near Cienega Gap. No subsequent seismic activity has been reported for this area.

A discontinuous zone of fault scarps offsetting Pleistocene alluvium (Qmo and Qm) were identified in the northwest corner of the map area, just northeast of Corona de Tucson. These scarps are the northern extension of the Santa Rita fault zone, previously identified along the western side of the Santa Rita Mountains for about 35 miles (60 km) from Tubac to Corona de Tucson (Pearthree and Calvo, 1987). Scarps in the Santa Rita fault zone trend northeast to north-south and are 1 to 6 km west and northwest of the base of the Santa Rita Mountains. Scarps range up to about 5 m in height and have maximum slope angles up to about 10°. Surficial deposits as young as late Pleistocene are displaced but latest Pleistocene and Holocene deposits are not faulted, which brackets the age of youngest faulting between 10-20 ka and 75-130 ka. Quantitative analysis of fault scarp morphologies indicates that the youngest surface rupture occurred between about 60-130 ka (Helmick, 1986; Pearthree and Calvo, 1987). In the central part of the fault zone, displacement of late Pleistocene surfaces averages about 2 m, in contrast to 4 to 5 m of displacement of middle and early Pleistocene surfaces. Using surface displacement estimates and various estimates of surface rupture length, Pearthree and Calvo (1987) concluded that two paleoearthquakes of magnitude 6 ¾ to 7 ¼ occurred along the Santa Rita fault zone in the past 200 to 300 ka. Helmick (1986) also concluded two periods of surface rupture based on profile analysis using a diffusion-equation model derived from the continuity equation for hillslope degredation.

A profile from a scarp displacing a Qm surface in the map area was analyzed to estimate morphologic age using a program developed by Ramon Arrowsmith (Arizona State University, personal communication) based on a diffusion-equation model. The morphological age of the scarp, based on this program, was 117 ka, with an error interval of 84-160 ka. Although this age generally agrees with previous findings, displacement of this scarp was about 5 meters, which may indicate two events. Thus, the reported scarp age estimate likely reflects some combination of total scarp age (the age of the first faulting event) and the age of the youngest faulting event. Geophysical investigations on the northern part of the fault zone indicate that that part of the fault dips gently to the northwest (Johnson and Loy, 1992). This implies that the area of the seismogenic fault may be larger than previously suspected, and that it dips beneath the Tucson metropolitan area.

The evidence of low frequency Quaternary fault activity combined with the existence of broad bedrock pediments on the west side of the Santa Rita Mountains indicates that the long-term slip rate on the Santa Rita fault zone is very low. The very long recurrence intervals between surface ruptures and evidence for very low long-term slip rates are consistent with other Quaternary fault zones that have been studied in southeastern Arizona, southwestern New Mexico, and northern Sonora (Pearthree, 1986; Bull and Pearthree, 1988; Demsey and Pearthree, 1994; Pearthree, 1998). The fault activity that is observed in this region is either a late pulse of activity related to the Basin and Range disturbance or a new, weakly extensional tectonic regime that has developed in the middle to late Quaternary.

STRATIGRAPHY

Paleozoic Units

Paleozoic units in the study area are complexly deformed and in many areas the carbonate rocks are coarsely recrystallized marble. The layer cake stratigraphic succession established in homoclinal sequences of the southern Empire Mountains (Finnell, 1971) is difficult to correlate with the dismembered and altered slivers of limestone and siliciclastic strata in the northern part of the range. In many areas, the all-inclusive map unit, Paleozoic limestone (¼l) had to be employed. A few outcrops of deformed lower Paleozoic rocks in the northernmost Santa Rita Mountains were not examined during this study.

Mesozoic Units

Gardner Canyon Formation

The oldest Mesozoic unit in the map area is the Gardner Canyon Formation (J ² g), which consists of a sequence of red mudstone (now slate) with variable amounts of interbedded volcaniclastic sandstone, pebbly sandstone, and conglomerate. Volcanic flows are present and mappable in two isolated areas. A fine-grained, crystal-poor dacitic lava or tuff (J ² gp) is present along the western edge of the easterly adjacent Narrows map area (Spencer et al., 2001), and in this map area, a 15 meter-thick sheet of crystal-rich dacite tuff (J ² d) is interbedded with red mudstone and volcaniclastic rocks. The upper and lower contacts of the Gardner Canyon Formation are typically disrupted by low-angle faults, but not all exposures of the unit have been studied. In some areas, it appears that volcaniclastic strata of the Gardner Canyon Formation may grade upwards into basal conglomeratic rocks of the Glance Conglomerate, the lowest stratigraphic division of the Bisbee Group.

Marvin et al. (1973) report widely disparate Pb alpha ages of 170 $\pm$ 35 Ma for a rhyolitic tuff from the Gardner Canyon Formation in the easterly adjacent Narrows quadrangle (Empire Mountains), and 210 $\pm$ 30 Ma for a rhyolitic welded tuff in the Santa Rita Mountains (southerly adjacent Empire Ranch quadrangle). The crystal-rich dacitic tuff we sampled along the east-central edge of this map area has not been dated. A large sample of this rock (sample FK-2293, UTM location: 534761E, 3532971N) was submitted to Nancy Riggs at Northern Arizona University for U-Pb dating.

Bisbee Group

The basal unit of the Bisbee Group, the Glance Conglomerate (KJg), varies greatly in thickness and composition across the study area. In the Empire Mountains, where it overlies Paleozoic units, the Glance Conglomerate consists of coarse-grained, massive conglomeratic rocks that thin rapidly to the south. Finnell (1970) estimated that the Glance Conglomerate is over 1500 meters thick in some areas, and suggested that the unit could be subdivided based on the dominant clast type, even though this was not done on his map of the area (Finnell, 1971). We recognized monolithic conglomerate units composed of limestone clasts (KJgl), quartzite clasts (KJgq), and granitiod clasts (KJgg) in the map area, as well as a unit consisting of quartzite and granite clasts (KJgqg) in the easterly adjacent Narrows map area (Spencer et al., 2001). In general, the older conglomerate units consist of clasts derived from the youngest (carbonate) units (Finnell, 1970). These variations are interpreted to represent the sequential unroofing of progressively deeper stratigraphic levels of an uplift directly to the north of the thick wedge of conglomerate.

Just to the north of the north end of the Empire Mountains, where it directly overlies Proterozoic basement, the Glance Conglomerate consists of a relatively thin sequence of arkosic sandstone and monolithic granitoid-clast conglomerate. Locally, some of this conglomerate includes lenses with abundant carbonate-clasts.

In the vicinity of the study area the Glance Conglomerate is overlain by a siliciclastic sequence dominated by shale and siltstone with sparse beds of limestone (Tyrell, 1957; 1965, Archibald, 1987, Finnell, 1970, Hardy, 1997). These rocks are divided into four formations, from older to younger; Willow Canyon (900 meters), Apache Canyon (450 meters), Shellenberger Canyon (1,200 meters), and Turney Ranch (1,000 meters) formations (thicknesses according to Finnell, 1970). The older three formations consist of arkosic to feldspathic and rarely quartzose sandstone and pebble conglomerate and chert granule sandstone to pebble conglomerate interbedded with dark olive gray shale and siltstone. The sandstone is commonly pyritic and typically has argillaceous matrix. The sandstone and conglomerate display bed-scale bed forms (chiefly cross-stratification) and Bouma (1962) sequence sedimentary structures. The sequence also includes limestone beds, locally abundantly, containing fresh water molluscan shell fragments. Some sequences, near the base, also include abundant silicified wood fragments up to 2 meters in length.

The Willow Canyon, Apache Canyon, and Shellenberger Canyon formations represent a monotonous sequence that intertounges to the north with a thick wedge of Glance Conglomerate (Finnell, 1970). The sequence is interpreted as a marginal lacustrine, alluvial, and distributary channel sequence with some deeper water turbidite successions. The formation boundaries are defined by distinctive sequences (Tyrell, 1957; 1965, Archibald, 1987, Finnell, 1970, Hardy, 1997) that can be identified in the homoclinal sections exposed in the southern Empire and Whetstone mountains, but in areas of poor, discontinuous exposure and structural complexity we found that it is not feasible to assign formation names to individual outcrops. The petrography and sedimentology of the sandstone and shale in the lower three formations are very difficult to differentiate, and for this reason we were obliged to lump all three formations together as one map unit (Kb).

The youngest unit of the Bisbee Group, the Turney Ranch Formation, is distinctively different from the older three and was recognized as a separate map unit (Kq). The Turney Ranch Formation consists of quartzose sandstone characterized by bed-scale bed forms (Bouma [1962] sequences notably absent) that are interbedded with oxidized, reddish siltstone and shale. Detailed petrographic studies of the Bisbee Group in this area show that the Turney Ranch Formation is significantly more quartzose than the other older formations of the Bisbee Group (Klute, 1991, p. 167-176). In this study area, the Turney Ranch Formation is interpreted as a purely alluvial succession.

The Turney Ranch Formation is not known to intertongue with the Glance Conglomerate. In the south, it overlies at least 2,000 meters of older Bisbee Group strata, but in the north, in a synclinal keel that rises out of the piedmont just to the south of I-10, only 0-100 meters of feldspathic, argillaceous sandstone of the Kb map unit is present between the Turney Ranch Formation and a thin sequence of Glance Conglomerate. Just to the north of this keel (between I-10 and Cienega Creek), the Kb unit thickens dramatically (Richard et al., 2001; Spencer et al., 2001).

It is important to clarify that the boundaries of our three main divisions of the Bisbee Group (Glance Conglomerate, a combined Willow Canyon – Apache Canyon – Shellengerger Canyon (Kb) unit, and a quartzose sandstone and red shale unit (Kq) roughly equivalent with the Turney Ranch Formation) may not correlate with the sequence boundaries used by other geologists in southerly adjacent areas of the Santa Rita, Empire, and Whetstone mountains. The upward transition into the Turney Ranch is somewhat arbitrary, and we may have included much of what others call Shellenberger Canyon Formation in our Kq map unit. Conversely, we may have placed some of the Turney Ranch Formation into our Kb unit. In the Mount Fagan quadrangle, exposure of the Bisbee Group is poor, and the rocks are typically intensely fractured, folded and faulted. Many exposures are isolated and marker beds are difficult to trace over long distances. We emphasize that our map units are informal, and although it appears that our nomenclature may be a step backwards in our understanding of the Bisbee Group in the Mount Fagan quadrangle relative to the work of Finnell (1970; 1971), we found it to be the only way to portray these units without creating meaningless and misleading contacts. We have however included all of the contacts that were mapped between the Willow Canyon, Apache Canyon, and Shellenberger Canyon formations by Finnell (1971) on our map as marker beds (Plate 1).

Our ability to assign the four part nomenclature of the Bisbee Group that has been applied elsewhere (Tyrell, 1957, 1965; Finnell, 1970, 1971) was also seriously hampered by our inability to examine large areas of Bisbee Group exposures in the northern Santa Rita Mountains. Of particular importance is the discovery of a thin, widespread rhyolite ash-flow tuff sheet within the Bisbee Group in the southern Narrows quadrangle (Spencer et al., 2001) that hopefully can be used as a time-stratigraphic marker unit in the structurally complex areas of the northern Santa Rita and Empire mountains.

Freshwater bivalves and gastropods were collected from two locations in the Willow Spring – Apache Canyon – Shellenberger Canyon lithofacies of the Bisbee Group (sample localities 3-22-01-01 SMR [Bootlegger Spring; SE ¼, SW ¼, sec. 31, T. 17 S., R. 18 E.] and 3-8-01-01 SMR [700 m south-southeast of Fleming Tank; NE ¼, NW ¼, NE ¼, sec. 27, T. 17 S., R. 17 E.]). Both localities contain gastropods of the genera Viviparus and Reesidella, and the Fleming Tank locality yielded unionid bivalves. The Bootlegger Spring locality yielded the bivalve Musculiopsis russelli, which has also been reported in the Apache Canyon Formation in the Whetstone Mountains (Scott, 1987; see also Yen, 1951). These fossils were identified by Spencer G. Lucas (Curator of Paleontology and Geology, New Mexico Museum of Natural History, Albuquerque), and are "no older than Barremian" and "no younger than Aptian" (Spencer Lucas, written communication, 2001). The Fleming Tank locality is near the base of the Willow Spring – Apache Canyon lithofacies of the Bisbee Group, whereas the stratigraphic position of the Bootlegger Spring locality within the Willow Spring – Apache Canyon lithofacies of the Bisbee Group is not known because of structural disruption and lack of stratigraphic markers in the area (Spencer et al., 2001).

Upper Cretaceous

<u>Fort Crittenden Formation and andesitic lava of the Salero Formation</u>

The Bisbee Group is overlain with significant angular unconformity by a thick succession of massive, clast-supported, quartzite clast, boulder-cobble conglomerate and pebbly sandstone of the Fort Crittenden Formation (Kfc). The Fort Crittenden Formation is in turn overlain by a thick pile of mafic to intermediate lava flows (Ka), much of which contains abundant evidence of deposition in a subaqueous envirnonment. Pillow breccia, hyaloclastite, and hyaloclastite breccia are abundant throughout the lower portion of the unit on the west slope of Mount Fagan. On the east, the andesite lava is overlapped by a dacitic lava unit (Kdl). In one area, along the southwest edge of the map area, a finer-grained sequence of Fort Crittenden Formation (Kfcf) conglomerate grades upwards into a heterolithic breccia (Kfcv) containing angular to sub-angular clasts of andesitic lava and rounded clasts of quartzite. This relationship suggests that the Fort Crittenden Formation was overlain without significant hiatus by the volcanic rocks of the basal Salero Formation. Additional evidence, discussed in the next section, also suggests that the Fort Crittenden Formation was still relatively wet and plastic during eruption of the next youngest volcanic unit, the rhyolite of Mount Fagan.

<u>Rhyolite of Mount Fagan, Salero Formation</u>

Andesitic lava of the Salero Formation is overlain by thick pile of silicic ash-flow tuff, herein called the rhyolite of Mount Fagan (Kr). At one locality on the south flank of Mount Fagan, about 20 meters of an older, welded, crystal-rich, dacite ignimbrite (plagioclase and biotite phenocrysts) overlies the andesite. Everywhere else, the andesite lava is overlain by the rhyolite of Mount Fagan, a crystal-rich, plagioclase, quartz, K-feldspar-phyric ash-flow tuff. One sample of the rhyolite of Mount Fagan from near the crest of Mount Fagan was submitted to Bill McIntosh at the New Mexico Geochronological Laboratory in Socorro for possible dating ^{40}Ar/^{39}Ar dating of its K-feldspar phenocrysts (sample FK-3277, UTM location: 526352E, 3528477N).

The rhyolite of Mount Fagan is present throughout the Santa Rita Mountains and portions of the northern piedmont of the Empire Mountains, and in all of these areas it contains very large lithic blocks and swarms of lithic blocks composed of older units, principally the andesite lava (Ka), Fort Crittenden Formation (Kfc), and Bisbee Group (Kb and Kq). In many areas, lithic blocks exceed several hundred meters in diameter, and in one area in the south, lithic blocks of intact sequences of older strata are preserved as elongate slabs up to 300 meters thick and over a kilometer in length. Zones of the rhyolite of Mount Fagan which contain lithic fragments make up more than 75% of the unit in the map area. Several map units of lithic breccia are recognized. Mesobreccia (Krz) consists of matrix-supported rhyolite tuff with heterolithic clasts generally less than 1 meter in diameter. Megabreccia (Krg) consists of matrix-supported or clast-supported rhyolite tuff with very large (1 to >300 meters) heterolithic lithic clasts. The megabreccia is further divided into monolithic varieties; andesite (Kra), Fort Crittenden Formation (Krc), Turney Ranch lithofacies (Krq), and Willow Canyon – Apache Canyon – Shellenberger Canyon lithofacies (Kb). Minor zones of limestone megabreccia (Krl) derived from Paleozoic limestone units are also present along the eastern edge of the preserved outcrop belt.

Spectacular monolithic megabreccia slabs in the southern part of the map area must represent the catastrophic collapse of an oversteepened cauldron margin where a huge chunk of intact pre-cauldron strata was pitched into the cauldron and only partially disaggregated before the elongate slabs, some of which preserve stratigraphy, were encased in the surrounding rhyolite ash-flow tuff. Close examination of these blocks show a myriad of anfractuous dikes and blebs of the host rhyolite ash-flow tuff infiltrating along contacts with adjacent mezobreccia (Krz) or lithic-poor ignimbrite (Kr). Slabs and blocks of the monolithic Bisbee Group megabreccia (Krb and Krq) are typically so internally shattered that primary contacts between individual sandstone and argillite beds are rarely preserved. However, megabreccia blocks of the Fort Crittenden Formation are remarkably well preserved, with only minor fracturing and disruption of bedding features. We speculate that this difference in degree of shattering indicates that the Fort Crittenden Formation was poorly lithified when it collapsed into the cauldron and so absorbed the seismic energy associated with collapse without pervasive fracturing. The Bisbee Group, which was folded, metamorphosed and eroded prior to Fort Crittenden Formation deposition was already strongly lithified and so may have been prone to fracturing during caldera formation.

Volcanic-tectonic depressions

Andesitic lava depression

The andesitic lavas at the base of the Salero Formation fill a 1-2 kilometer deep, northwest-striking trough that appears to be a half-graben. The northeast side of the paleotrough was mapped as a fault by Finnell (1971). Although possibly faulted in some areas, we believe the contact to be largely depositional, and overlapped by the volcanic rocks. We interpret the trough-bounding fault to be concealed and suggest that its buried trace can be approximated by the trace of a prominent, nearly vertical, northwest-striking quartz porphyry dike (Plate 1). The dike runs at a slightly oblique angle to the contact, and moves away from the contact with increasing depth. Towards the bottom of the trough, andesitic lava is intruded by probable intrusive bodies of similar composition (these intrusions were not mapped separately). Although not a caldera, this elongate basin appears to be a volcano-tectonic depression. The probable continuation of the trough-bounding fault zone to the southeast is the major northwest-striking fault mapped by Finnell (1971) in the southwest corner of the map area. The trace of the fault appears to be offset to the north about 1 kilometere across the northwest-side-down, mid-Tertiary Davidson Canyon fault zone (as it should be for a southwest-dipping structure). The northwest-striking fault zone mapped by Finnell (1971) in the southern Empire Mountains is not associated with any hypabyssal rocks, so it would appear that the fault zone was not everywhere associated with volcanism.

Mount Fagan Cauldron

Since all exposures of Mount Fagan rhyolite in the map area are of intracauldron facies, it is difficult to define any caldera margins. The fact that rhyolite of Mount Fagan is not present in the Empire Mountains block is meaningless since the part of the section that might include these rocks is not exposed. There is however, some evidence that a west-facing caldera margin was located along the mid-Tertiary, west-side-down Davidson Canyon fault zone that separates the Empire Mountains from the Santa Rita Mountains. Intracaldron megabreccia blocks composed of Paleozoic limestone are present only along the eastern edge of the hanging wall of this fault, and the fault zone is characterized by strands that are intruded by the Upper Cretaceous Empire Mountains stock. Since this stock, and a pair of similar stocks in the northern Santa Rita Mountains seem likely candidates for being part of a subcaldera pluton, it is possible that the intruded faults along the Davidson Canyon fault zone are related to caldera formation.

Pantano Formation

Definition

Along the northern edge of the map area, folded Mesozoic sedimentary rocks of the Bisbee Group are overlain with angular unconformity by the Pantano Formation (Finnell, 1970), a thick succession of fanglomerate with lesser amounts of mudstone, limestone, and volcanic rocks. These rocks thicken rapidly to the north of the crystalline basement – Bisbee Group block which makes up the northern piedmont slopes of the Empire Mountains. Excellent exposures of east-tilted conglomerate, andesite lava and mudstone are preserved in deep road cuts of I-10 between the Sonoita Highway (Exit 281) and Marsh Station (Exit 289) exits. The first detailed description of these rocks (Brennan, 1957) failed to recognize the many fault repeats of this sporadically well-exposed section, and concluded that over 4 kilometers of section with multiple flows of andesite lava were present. Balcer (1984) recognized multiple normal faults, and defined a stratigraphic framework based on a single medial andesite unit and concluded that the sequence, although still quite thick, was significantly thinner. We concur with Balcer's (1984) observations, with minor changes, and assign informal names to the principle units.

As originally defined (Finnell, 1970) and as suggested by Balcer (1984), the Pantano Formation includes only the older part of a complex Mid-Tertiary sequence in the Cienega Gap area. Younger sedimentary rocks in the basin were assigned to the Nogales Formation (Drewes, 1977), but since this unit is defined in a separate basin over 60 kilometers to the south, we do not use this term. Instead, we refer to these rocks as the conglomerate of Agua Verde Creek and the unit of Wakefield Canyon. The unit of Wakefield Canyon overlies the Pantano Formation just to the east of this map area along a pronounced angular unconformity in a prominent ridge that crosses I-10 just west of the bridge of Cienega Creek (Spencer et al., 2001).

Only the Pantano Formation is present in the Mount Fagan quadrangle. For a detailed description of the complex facies relationships in the younger two sedimentary sequences, see Spencer et al. (2001).

Stratigraphy and petrology

The Pantano Formation is divided into upper (670 meters) and lower divisions (730 meters) by a distinctive, coarsely plagioclase porphyritic andesite lava flow. The andesite lava has been dated at 24.9 ± 5.2 Ma (K/Ar plagioclase date with 2s uncertainty [95% confidence interval]), and a sample from the northeastern Rincon Mountains (Mineta Ridge) yielded an age of 26.9 ± 4.8 Ma (2s uncertainty [95% confidence interval]; Shafiqullah et al., 1978). Andesite lava with similar compostion and distinctive coarsely porphyritic texture elsewhere in southern Arizona have been correlated as part of the same regional effusive event. Dates of flows elsewhere (Percious, 1968) are similar to those in the Cienega Gap area. The andesite lava (Ta) within the Pantano Formation is typically overlain by a thin volcaniclastic and pyroclastic sequence (Tas). Locally, in the northerly adjacent Vail map area (Richard et al., 2001) the porphyritic andesite is overlain by a fine-grained andesite lava (Tap).

Although dominated by coarse-grained conglomerate and pebbly sandstone, the basal lower Pantano Formatio consists of a fine-grained sequence including mudstone, thin-bedded sandstone and abundant thin- to medium-bedded, quartz sandy pisoid packstone limestone beds (Tpfl). This fine-grained subdivision of the lower Pantano Formation is difficult to distinguish from the finer grained portions of the upper Pantano Formation. In some areas to the north and east (Richard et al., 2001; Spencer et al., 2001) where age relationships with the andesite lava (Ta) are uncertain, fine-grained facies of the Pantano Formation are undifferentiated (Tpf).

The upper Pantano Formation is in general finer grained than the lower Pantano Formation, and it also tends to fine towards the north. Balcer (1984) referred to this division as the "mudstone member", but since its dominant lithology is pebbly sandstone and cobble-pebble conglomerate we refer to these strata as upper Pantano Formation. In the easterly adjacent Rincon Peak – Narrows map area (Spencer et al., 2001) at least one thin nonwelded felsic tuff (Tt_1) is present near the base of the upper Pantano Formation, and five samples of this tuff (all from the easterly adjacent Narrows quadrangle) have been submitted to Bill McIntosh at the New Mexico Geochronological Research Laboratory in Socorro for dating (samples with UTM locations: FK-1336 [539119E, 3538719N], FK-1702 [539631E, 3536448N], FK-1706 [539583E, 3536176N], FK-1707 [539544E, 3536242N], and FK-1832 [539633E, 3535660N]).

Clasts in the Pantano Formation south of Cienega Creek consist mostly of Bisbee Group sandstone, siltstone, and argillite (Kb, and Kq map units), crystal-rich quartz porphyry (Tq map unit), and crystal-rich welded rhyolite tuff (Kr map unit). Since these three rock types constitute at least 90% of the bedrock exposure in the northern Santa Rita Mountains, we interpret this as the probable source area for the Pantano Formation. However, Balcer's (1984) paleocurrent measurements in the Pantano Formation are mostly westerly for the lower division and northeasterly for the upper division. Clasts of limestone and granitoid clasts are also present but are very sparse. By contrast, the next younger unit in the area, the unit of Wakefield Canyon, contains abundant granodiorite clasts and a significantly greater amount of Paleozoic limestone clasts.

Tectonic history of the Pantano basin

The base of the Pantano Formation in the northern Empire Mountains and Cienega Creek area is marked by two units; a 33.01 ± 0.38 Ma (Ar/Ar single crystal sandine, McIntosh and Peters, personal communication) rhyolite ash-flow tuff that typically directly overlies folded Bisbee Group, and a sequence of lacustrine strata (Tpfl) including pisoid packstone limestone and abundant mudstone. Gently dipping eutaxitic foliation in the welded tuff is typically discordant with respect to bedding in the overlying sedimentary rocks and the tuff is not considered part of the Pantano Formation (Balcer, 1984). The orientation of the foliation in the welded tuff after restoration of approximately 40 degrees of easterly dip of the basal Pantano Formation is west-dipping, and suggests that these fault blocks may undergone a phase of westerly tilting prior to deposition of the Pantano Formation. Paleomagnetic analysis of the welded tuff may help determine if the eutaxitic foliation represents original horizontal for this Oligocene unit, and shed some light on the intriguing possibility of an older tilt history.

Locally, a thin sheet of red, clast-supported conglomerate occurs at the base of the Pantano Formation, but the basal contact of the Pantano Formation is preserved in only two areas; an east-striking contact in the footwall of a north-side down fault in the northeast corner of the map area, and a north-striking contact at the base of a major, younger, east-tilted fault block just to the northeast this map area. The east-tilted fault block is bounded by a strand of the Davidson Canyon fault, a west-side-down fault with at least 2,000 meters of offset that clearly cuts the previously mentioned north-side-down fault and the Pantano Formation. The north-side-down fault appears to have been active during and after deposition of the lower Pantano Formation, but appears to be overlapped by the upper Pantano Formation (Plate 1). Farther east, similar relationships occur that suggest significant thickening of the lower Pantano Formation from south to north across the fault, and possibly, complete overlap by younger parts of the upper Pantano Formation (Spencer et al., 2001).

Motion along the north-side-down fault that bounds the great thicknesses of Pantano Formation just south of I-10 was complete or nearly so, by the time of upper Pantano Formation deposition. Changes in style of sedimentation occurred abruptly at the base of the upper Pantano Formation, but this change from conglomerate dominated to sandstone-mudstone dominated might not be just because a thick sequence of lava flows damned some important drainages. Significant amounts of conglomerate were still shed into the basin during upper Pantano Formation time, but it seems that the basin had changed significantly.

A maximum of 20 degrees of fanning dips are recorded in the Pantano Formation along the I-10 corridor. Locally, this fanning is achieved with minor angular unconformities. Finnell (1970), recognized three major angular unconformities, but we concur with Balcer (1984), that these are not major features. To the south of Cienega Creek, major tilting of the Pantano Formation did not occur until after it was deposited. An apparently conformable sheet of monolithic limestone avalanche breccia within the uppermost upper Pantano Formation, south of Cienega Creek (Spencer et al, 2001) possibly represents the earliest evidence of catastrophic collapse of the footwall of the Rincon Mts detachment fault system to the north, and it may have heralded significant changes in the geometry of the Pantano basin. After this event, the basin was disrupted by numerous west-side-down normal faults that clearly cut through all of the Pantano Formation south of Cienega Creek. To the north of the creek, however, there is sparse evidence of these normal faults, and in the vicinity of Cross Hill (Spencer et al, 2001) an essentially horizontal sheet of mixed monolithic and polymict avalanche breccia buries a confusing sequence of gently tilted, but disrupted mudstone and sitltstone. It is not know if these mudstone beds are part of the upper Pantano Formation, part of the unit of Wakefield Canyon, or both. To the south of Cienega Creek, and well to the east in the Mescal quadrangle (Skotniki, 2001) strata of the unit of Wakefield Canyon clearly overlap Pantano Formation strata with pronounced angular unconformity. North of Cienega Creek, however, the unit of Wakefield Canyon, conglomerate of Aqua Verde Creek, and the upper Pantano Formation may interfinger, and tilting of all of these strata may never have been severe.

Clasts of mylonitized granitoids do not appear until deposition of the youngest unit of the Pantano Formation, the Aqua Verde Creek facies which is found well to the northeast of Cienega Creek and along the southern flank of the Rincon Mountains detachment fault (Spencer et al, 2001).

STRUCTURAL GEOLOGY

Bisbee trough

The late Jurassic to middle Cretaceous Bisbee Group of southeastern Arizona and adjacent parts of New Mexico, Sonora, and Chihuahua, was deposited in a structurally complex rift trough produced by late Jurassic rifting. This rifting occurred in an area that had previously been subject to Jurassic, subduction-related magmatism (Bilodeau et al., 1987; Dickinson et al., 1987, 1989). In the Mount Fagan area, movement on a major south-facing normal fault or fault system was probably responsible for a clastic wedge of conglomerate deposited in a graben or half-graben along north edge of the Empire Mountains. The resulting basin is referred to as the Empire Mountains sub-basin of the Bisbee trough. Analyses of sparse basaltic lava flows near the base of the Bisbee Group in the study area and adjacent areas (see also Hardy, 1997, and Spencer et al., 2001) may provide some insight into the tectonic setting of the Bisbee trough.

Laramide deformation

Geometry

Two phases of Laramide compressional deformation are evident in the map area. The best evidence for multiple deformation is in the northwest corner of the easterly adjacent Narrows quadrangle, where a tight to isoclinal synclinal keel of Bisbee Group is folded about a broad, open, east-plunging antiform (Spencer et al., 2001). In the central Mount Fagan quadrangle, a large area of Bisbee Group mapped by Finnell (1971), is interpreted as a regional, tight to isoclinal anticline folded about a broad, open, east-plunging syncline.

The orientation of the younger folds is, in general, east-west, but since the older folds have been deformed, their original orientation is more difficult to determine. Complex structures in the northern Empire Mountains can also be interpreted in terms of two compressional events. A west-vergent thrust placing complexly faulted slivers of Permian sandstone and limestone over Jurassic-Triassic Gardner Canyon Formation is present at the north end of the range. Note that the apparent steepening of this thrust to the north is interpreted as a lateral ramp in the thrust sheet. The direction of thrusting is interpreted to be to the west-southwest based on the orientation of a pervasive slatey cleavage in mudstone of the Gardner Canyon Formation. Farther to the south, a south-plunging anticline developed in middle Paleozoic rocks is cut by a south-dipping thrust fault. Another south-plunging anticline is developed in Bisbee Group rocks in the hanging wall of the Davidson Canyon fault farther to the south and is possibly a continuation of the anticline in the Paleozoic rocks.

The south-plunging folds and the west-vergent thrust in the Empire Mountains are tentatively correlated with the older phase of folding of the Bisbee Group in the foothills of the Santa Rita Mountains in on the northern piedmont of the Empire Mountains. The south-dipping thrusts in the Empire Mountains are tentatively correlated with the younger phase of east-west striking folds. One of these south-dipping thrusts is the relatively minor fault that cuts the folded Paleozoic rocks just to the north of the Empire Mountains stock. The most important south-dipping, north-vergent fault of the younger phase is the controversial range-bounding fault along the northern edge of the Empire Mountains. This fault was originally interpreted as a south-vergent, north-dipping fault by Bilodeau (1979) and Bilodeau et al. (1987) that coincidentally cut through the south-dipping normal fault zone that bounds the north flank of the Empire Mountains sub-basin of the Bisbee trough. We prefer a north-vergent, south-dipping geometry for this fault for five important reasons: 1) the map pattern, although in areas of subdued topography, suggests a southerly dip. 2) a synclinal keel of Bisbee Group just to the north is asymmetric with a steeper southern limb. 3) the apparent offset of the fault across the west-side-down Davidson Canyon fault is to the north, consistent with a southerly dip. 4) the other east-west striking thrust fault in the Empire Mountains dips to the south. 5) a southerly dip is consistent with reactivation of the major south-dipping paleoescarpment and fault zone that bounds the northern flank of the Empire Mountains sub-basin of the Bisbee trough. Reactivation of this fault would account for the reduction of large amounts of south-side-down stratigraphic offset that must have occurred during formation of the Bisbee trough, whereas the interpretation of Bilodeau (1979) and Bilodeau et al. (1987) would increase the amount of offset.

Regional significance

The orientation of the younger, east-west striking compressional Laramide event seems to have been influenced by the east-west striking, south-dipping orientation of the basement faults related to formation of the Jurassic-Early Cretaceous Bisbee trough. The older phase of folding appears to have been oriented in more of a north-south direction.

Age

The age of Laramide folding in the area is constrained between the age of the uppermost Bisbee Group (Lower Cretaceous?) and the age of the basal Fort Crittenden Formation which is older than the approximately 75 Ma Corona de Tucson stock which intrudes Fort Crittenden Formation in the Santa Rita Mountains. The Fort Crittenden Formation overlies folded Bisbee Group with pronounced angular unconformity in a number of localities. The contact metamorphic aureole related to the ~72 Ma Empire Mountains stock is clearly post-kinematic with respect to axial planar cleavage in the south-plunging anticline developed in Paleozoic rocks along the east-central edge of the map area.

Late Cretaceous faulting

Emplacement of a thick sequence of andesitic lava of the basal Salero Formation was associatied with formation of a major, northwest-striking, half-graben and southwest-side-down normal fault that transects the southern third of the study area. Although associated with volcanism in the Santa Rita Mountains and overlapped by volcanic rocks of the Salero Formation, the apparent continuation of this fault in deeper structural levels of the Empire Mountains to the southwest is not associated with dike swarms or other plutonic rocks that might be associated with the volcanism. The fault is approximately parallel to northwest-striking faults that transect the Santa Rita Mountains farther south and continue as far to the southeast as the Huachuca Mountains. The nearest fault of similar orientation is the Sycamore Canyon fault directly to the southwest of the map area which Hardy (1997) interpreted as an oblique, sinistral, north-vergent reverse fault.

Mid-Teritary faults

The Santa Rita and Empire mountains are separated by the west-side-down Davidson Canyon fault zone. In the northeast corner two major west-side-down faults with a combined offset of at least 3,000 meters cut the mid-Tertiary Pantano Formation and these faults can be traced south-southwest for several kilometers across the peidmont, but from here it is not clear where they extend to the south. The western fault's trace is concealed by alluvium, but the eastern fault was traced across the poorly exposed northern pediment of the Empire Mountains by assuming that all exposures of the rhyolite of Mount Fagan are in its hanging wall. This approach produces a somewhat irregular map pattern. Farther south, the fault is assumed to coincide with an important west-side-down fault that cuts through the Empire Mountains stock along the west flank of the range. Finnell (1971) interpreted this fault to be intruded by the stock, but we found that, although some strands appear to be intruded by the stock, a main strand clearly cuts the stock. We interpret the younger strand(s) of the fault zone to be related to motion on the Davidson Canyon fault zone, and the intruded fault strands to be related to collapse of the caldera which erupted the rhyolite of Mount Fagan. The presence of a west-facing caldera margin of Upper Cretaceous age in this area may have influenced the location of the Davidson Canyon fault.

Cryptic low-angle faults and reactivated fault slivers

Several low-angle faults of unknown origin are present along Davidson Canyon and near Davidson Spring just west of the north end of the Empire Mountains. The faults might be related to Laramide thrusting, rhyolite of Mount Fagan cauldron formation, or mid-Tertiary extension, or all of these. The low-angle fault in Davidson Canyon in the northern part of the study area dips gently to the east with highly deformed Bisbee Group in the hanging wall and Early Proterozoic granodiorite in the footwall. In some areas, a fine-grained microbreccia that appears to be volcanic in origin was mapped along the fault plane and interpreted as rhyolite of Mount Fagan mesobreccia. By restoring 50 degrees of mid-Tertiary easterly tilting, this fault would dip gently to moderately to the west and we tentatively interpret it as being related to caldera formation.

Reactivated faults are interpreted for two complex zones of faulting in the northeast part of the map area. One is directly northwest of the north end of the Empire Mountains and consists of thin slivers of Bisbee Group sandstone and limestone and Pinal Schist caught between large expanses of Early Proterozoic granodiorite. The other, west of Davidson Canyon in the SE ¼ of sec. 13, R16E, T17S, consists of a sliver of Early Proterozoic granodiorite caught between Bisbee Group on the south and Permain Epitaph Formation on the north. This kind of fault, where slivers of stratigraphic units not normally present between the units on either side, seems best explained by reactivation of a normal fault as a thrust or vice versa. Other faults of this type are also found in piedmont areas to the northeast of the Empire Mountains (Spencer et al., 2001) and lend credence to our interpretation that a major fault at the north end of the Empire Mountains formed as a Bisbee-aged, south-side-down normal fault and was later reactivated as a north-vergent thrust or reverse fault (e.g., Bilodeau, 2001).

ECONOMIC GEOLOGY

Mineral deposits are of fairly minor importance in the map area, and are restricted largely to the cuprite district in the northern foothills of the Santa Rita Mountains (Kieth et al, 1993). Mineralization in this area appears to be related to the emplacement of a dense swarm of quartz porphyry dikes and related small stocks. In the Empire Mountains, the Empire Mountains stock accounts for relatively large zones of contact metamorphic aureoles in lower Paleozoic limestone units, at least one of which has been quarried commercially for its marble. At the south edge of the stock multiple prospects are present in the country rock.

UNIT DESCRIPTIONS
Miscellaneous Units

d **Disturbed—**Areas that have been so profoundly disturbed by human activity as to completely obscure the preexisting natural surface or bedrock geology. This unit is used primarily where large amounts of fill were used to build the I-10 roadbed.

b **Undifferentiated bedrock.**

Surficial Geology
Piedmont Alluvium

Quaternary and late Tertiary deposits cover the most of the piedmont areas north of Mount Fagan and the Empire Mountains and extend onto older deposits of the Tucson Basin. This alluvium was deposited primarily by larger streams that head in the mountains. Smaller streams that head on the piedmont have eroded and reworked some of these deposits. Surficial deposits range in age from modern to early Pleistocene or Pliocene. Approximate age estimates for the various units are given in parentheses after the unit name. Abbreviations are ka, thousands of years before present, and Ma, millions of years before present.

Qy **Undifferentiated Holocene alluvium (< 10 ka)—**Unit Qy includes both Qy_2 and Qy_1 deposits. It is used where it was not possible, at a scale of 1:24000, to separately map Qy_1 and Qy_2 surfaces. Unit Qy consists of smaller incised drainages on the piedmont and more extensive young alluvial fans at the base of the piedmonts, toward the Tucson Basin. Soil development consists of cambic horizons over weak to moderate (stage I to II) calcic horizons. This map units includes units 3B and 4 of Pearthree and Calvo (1987).

Qy£ **Late Holocene alluvium (<2 ka)—**Unit Qy_2 consists of channels, low terraces, and small alluvial fans composed of cobbles, sand, silt and boulders that have been recently deposited by modern drainages. In upper piedmont areas, channel sediment is generally sand, pebbles and cobbles, with some boulders; terraces typically are mantled with sand and finer sediment. On lower piedmont areas, young deposits consist predominantly of sand and silt, and some cobbles in channels. Channels generally are incised less than 1 m below adjacent terraces and fans, but locally incision may be as much as 2 m. Channel morphologies generally consist of a single-thread high flow channel or multi-threaded low flow channels with gravel bars adjacent to low flow channels. Downstream-branching distributary channel patterns are associated with the few young alluvial fans in the area. In these areas, channels typically are discontinuous, with small, well-defined channels alternating with broad expansion reach where channels are very small and poorly defined. Local relief varies from fairly smooth channel bottoms to the undulating bar-and-swale topography that is characteristic of coarser deposits. Terrace typically have planar surfaces, but small channels are also common on terraces. Soil development associated with Qy_2 deposits is minimal. Terrace and fan surfaces are brown, and on aerial photos they generally appear darker than surrounding areas, whereas sandy to gravelly channels appear light-colored on aerial photos. Vegetation density is variable. Channels typically have sparse, small vegetation. Along the larger washes, vegetation includes mesquite, yuccas, acacias, smaller bushes and grass may also be quite dense. Smaller washes typically have palo verde, mesquite, large creosote and other bushes along them.

Qy¢ **Holocene alluvium (~2 to 10 ka)—**Unit Qy_1 consists of low terraces found at scattered locations along incised drainages and broad, minimally dissected alluvial fans. Qy_1 surfaces are slightly higher and less subject to inundation than adjacent Qy_2 surfaces. Surfaces are generally planar; local relief may be up to 1 m where gravel bars are present, but typically is much less. Qy_1 surfaces are less than 2 m above adjacent active channels. Surfaces typically are sandy but locally have fine, unvarnished open gravel lags. Qy_1 surfaces generally appear fairly dark on aerial photos, but where a gravel lag is present, surfaces are light colored. Channel patterns on alluvial fans are weakly integrated distributary (branching downstream) systems. Qy_1 soils typically are weakly developed, with some soil structure but little clay and stage I to II calcium carbonate accumulation (see Machette, 1985, for description of stages of calcium carbonate accumulation in soils)— Qy_1 terrace surfaces support mesquite, prickly pear, yucca, and smaller bushes. Qy_1 fans support scattered trees along channels, but creosote and other small bushes are dominant.

Qly **Holocene to late Pleistocene alluvium (0 to 130 ka)—**Broadly rounded alluvial fan surfaces approximately 1 m above active channels composed of mixed alluvium of late Pleistocene and Holocene age. Drainage networks consist of a mix of distributary channel networks associated with larger drainages and tributary channels associated with smaller drainages that head on Qly surfaces. Qly areas are primarily covered by a thin veneer of Holocene fine-grained alluvium (unit Qy), but reddened Pleistocene alluvium (unit Ql and rarely, Qm) is exposed in patches on low ridges, in roads, and in cut banks of washes. The Holocene surfaces usually are light brown in color and soils have weak subangular blocky structure and minor carbonate accumulation. Qly fans mainly support creosote bushes.

Ql **Late Pleistocene alluvium (~10 to 130 ka)—**

Ql£ latest Pleistocene member (~10 to 20 ka)

Ql¢ late Pleistocene member (~75 to 130 ka)

Unit Ql consists of slightly to moderately dissected relict alluvial fans and terraces found on the upper, middle and lower piedmont, and scattered within the mountains. Moderately to well-developed, slightly to moderately incised tributary drainage networks are typical on Ql surfaces. Active channels are incised up to about 2 m below Ql surfaces, with incision typically increasing toward the mountain front. Ql fans and terraces are commonly lower in elevation than adjacent Qm and older surfaces, but the lower margins of Ql deposits lap out onto more dissected Qm surfaces in some places. Ql deposits consist of pebbles, cobbles, and finer-grained sediment. Ql surfaces commonly have loose, open lags of pebbles and cobbles; surface clasts exhibit weak rock varnish. Ql surfaces appear light orange to dark orange on color aerial photos, reflecting slight reddening of surface clasts and the surface soil horizon. Ql soils are moderately developed, with orange to reddish brown clay loam to light clay argillic horizons and stage II calcium carbonate accumulation. Ql fans in the southeast corner of the quadrangle are derived from carbonate-rich sources. These fans typically are gray on aerial photographs, have stage III calcium carbonate accumulation, and are incised up to 4 m. On the piedmont north of Mount Fagan, Ql can be broken into older, Ql_1, and younger, Ql_2, members. Ql_1 soils have more clay, redder surface horizons, and generally more extensive drainage networks on them, reflecting their greater antiquity. Unit Ql_2 soils are dark brown (10YR 3/3 moist) and appear dark gray in aerial photograph. In general, the upper 1 m of Ql_2 soils are more effervescent than Ql1 soils. Unit Ql_2 is correlative with unit 2c of Pearthree and Calvo (1987). Dominant forms of vegetation include grasses, small shrubs, and mesquite.

Ql_2 fans have dense and very diverse vegetation, such as palo verde and mesquite trees, several species of shrubs and cacti, but very few annuals.

Qlp **Late Pleistocene alluvium over dissected pediment (~10 to 130 ka)—**Unit Qlp consists of thin, discontinuous Ql deposits over dissected pediment. Bedrock is typically exposed in, and sporadically between, washes. Unit Qlp is found within the mountains, typically at the headwaters of larger drainages.

Qml **Middle to late Pleistocene alluvium (~10 to 500 ka)—**Unit Qml consists of mixed hillslope colluvium and middle to late Pleistocene alluvium that has formed as valley fill along drainages in unit QTs. Deposits range in thickness and soil development.

Qm **Middle Pleistocene alluvium (~130 to 500 ka)—**Unit Qm consists of moderately dissected relict alluvial fans and terraces with strong soil development found throughout the map area. On the piedmont north of Mount Fagan, Qm alluvium is deposited on top of unit QTs, which is often exposed beneath Qm. Qm surfaces are drained by well-developed, moderately to deeply incised tributary channel networks; channels are typically several meters below adjacent Qm surfaces. Well-preserved, planar Qm surfaces are smooth with moderate to tightly packed pebble and cobble lags; surface color is reddish brown; rock varnish on surface clasts is typically orange or dark brown. More eroded, rounded Qm surfaces are characterized by scattered cobble lags with moderate to strong varnish, broad ridge-like topography and some carbonate litter on the surface. Well-preserved Qm surfaces have a distinctive dark orange color on color aerial photos, reflecting reddening of the surface soil and surface clasts. Soils typically contain reddened, clay argillic horizons, with obvious clay skins and subangular to angular blocky structure. Underlying soil carbonate development is typically stage III, with abundant carbonate through at least 1 m of the soil profile; indurated petrocalcic horizons are rare. Qm surfaces generally support grasses, mesquite, palo verde, yuccas, shrubs and ococtillo. Unit Qm in correlative with unit 2b of Pearthree and Calvo (1987).

Qmp **Middle Pleistocene alluvium over dissected pediment (~130 to 500 ka)—**Unit Qm_p consists of thin, discontinuous deposits of Qm over dissected pediment, or on as remanant terrace and fan deposits over bedrock in the mountains along Davidson Canyon.

Qmo **Middle to early Pleistocene alluvium (~500 ka to 2 Ma)—**Unit Qmo consists of very old, high, dissected alluvial fan remnants with moderately well preserved fan surfaces and strong soil development. Qmo deposits and fan surface remnants are scattered across the northern Mount Fagan piedmont, but are best preserved near the mountain front. Qmo surfaces typically are fairly smooth to broadly rounded. Qmo alluvium is deposited on top of unit QTs, which is often exposed on hillslopes beneath Qmo. Qmo deposits consist of cobbles, gravels and boulders, with sand and finer clasts. Well-preserved, planar Qmo surfaces are smooth with moderate to tightly packed cobble and boulder lags; surface color is dark red; rock varnish on surface clasts is strong and typically orange or dark brown. Qmo soils are dark red with well-developed, heavy clay argillic horizons. Stage III to IV calcic horizons are typical. Qmo surfaces are dominated by grass, mesquite, prickly pear, cholla, and ocotillo.

Qo **Early Pleistocene alluvium (~1 to 2 Ma).** Unit Qo consists of the oldest and highest alluvial fan remnants, and are found only at the extreme western edge of the map area. Deeply dissected fan surfaces are moderately well preserved with strong soil development. Qo surfaces typically are fairly smooth to broadly rounded. Qo deposits consist of cobbles, boulders, and sand and finer clasts. Stage III to IV calcic horizons are typical. Where surfaces are planar and well-preserved, red, heavy clay argillic horizons are typical. Qo surfaces are dominated by grass, small shrubs, and ocotillo. Qo surfaces record the highest levels of aggradation in the Tucson basin and are probably correlative with other high, remnant surfaces found at various locations throughout southern Arizona (Menges and McFadden, 1981; Pearthree and Calvo, 1987).

QTs **Early Pleistocene to late Miocene alluvium (1 to 10 Ma)—**Unit QTs consists of very old, deeply dissected and highly eroded alluvial fan deposits. QTs surfaces vary from highly eroded ridges and deep valleys near the mountains, with ridgecrests typically 10 meters above adjacent active channels, to broadly rounded ridges towards Cienega Creek. The thickness of QTs deposits is not known. They are drained by deeply incised tributary channel networks. Even the highest surfaces atop QTs ridges are rounded, and original highest capping fan surfaces are not preserved. QTs deposits are dominated by gravel ranging from boulders to pebbles. Deposits are moderately to very strongly indurated and are quite resistant to erosion because of the large clast size and carbonate cementation. Soils typically are dominated by carbonate accumulation, which is typically stage V (cemented petrocalcic horizons with laminar cap) on ridgecrests. Carbonate litter is common on ridgecrests and hillslopes. On aerial photos, QTs surfaces are gray to white. QTs surfaces support creosote, mesquite, palo verde, ocotillo, and cholla.

Axial Stream Deposits

Sediment deposited by Davidson Creek is mapped separately. Surfaces consist of channels and terraces. Deposits are a mix of gravel and sand and finer material; older deposits are coarser than younger deposits; they exhibit mixed lithologies and a higher degree of rounding reflecting the large drainage areas of these streams.

Qycx **Modern river channel deposits (< 100 years)—**This unit consists of river channel deposits of Davidson Creek. It is composed primarily of sand and gravel. Above the junction with Cienega Creek, modern channels are typically entrenched several meters below adjacent young terraces. The current entrenched channel configuration began to evolve with the development of arroyos between 1880 and 1887 (Myrick, 1975; Dobyns, 1981), and continued to evolve through this century (Betancourt, 1990; Wood and others, 1999). Channels are extremely flood prone and are subject to deep, high velocity in moderate to large flow events.

Qy£x **Late Holocene river alluvium (< 2 ka)—**Unit Qy_{2r} consists of floodplains and low terrace deposits, and include Qyc_r deposits where they cannot be mapped separately. Qy_{2r} deposits are composed primarily of sand and gravel. Qy_{2r} surfaces will be inundated in large floods. Terraces typically have planar surfaces, but small channels are also common on terraces. Soil development associated with Qy_{2r} deposits is minimal. Unprotected channel banks formed in Qy_{2r} deposits are very susceptible to lateral erosion.

Qy¢x **Holocene river terrace deposits (2 to 10 ka).** Unit Qy_{1r} consists of low terraces flanking the main channel along Davidson Creek. Terrace surfaces are flat and uneroded, except immediately adjacent to channels. Qy_{1r} deposits consist of weakly to unconsolidated sand, silt, and clay. Soils are weakly developed, with some carbonate filaments and fine masses and weak soil structure in near surface horizons. In upper Davidson Canyon, Qy_{1r} surfaces may experience sheetflooding during large floods in areas where the main channel is not deeply entrenched, and as a result of flooding on local tributaries that debouch onto Qy_{1r} surfaces.

Ql^{x} **Late Pleistocene river terrace deposits (10 to 130 ka)—**Unit Ql$_r$ consists of remnant river terrace deposits along Davidson Creek. These terraces are typically 2 m above the active channel in upper Davidson Canyon to 10 m near the confluence with Cienega Creek. Ql$_r$ deposits consist of cobbles, gravels and finer-grained sediment. Ql$_r$ surfaces commonly have loose, open lags of cobbles and gravels; surface clasts exhibit weak rock varnish. Ql$_r$ surfaces appear light orange color aerial photos, reflecting slight reddening of surface clasts and the surface soil horizon. Ql$_r$ soils are moderately developed, with orange to reddish brown clay loam to light clay argillic horizons and stage II calcium carbonate accumulation. Vegetation on Ql$_r$ terraces consists of scattered mesquite, prickly pear and creosote bushes.

Qm^{x} **Middle Pleistocene river terrace deposits (130 to 500 ka)—**Unit Qm$_r$ consists of remnant river terrace deposits along Davidson Creek. These terraces are typically 4 m above the active channel in upper Davidson Canyon to 15 m near the confluence with Cienega Creek. Qm$_r$ deposits consist of cobbles, gravels and finer-grained sediment. Qm$_r$ surfaces commonly have loose, open to moderately packed cobbles and gravel surface lags; surface clasts exhibit moderate rock varnish. Qm$_r$ surfaces appear in orange color aerial photos, reflecting reddening of surface clasts and the surface soil horizon. Soils typically contain reddened, clay argillic horizons, with obvious clay skins and subangular to angular blocky structure. Underlying soil carbonate development is typically stage III, with abundant carbonate through at least 1 m of the soil profile; indurated petrocalcic horizons are rare. Dominant vegetation includes mesquite and prickly pear cactus with fewer creosote bushes than Ql$_r$ terraces.

Hillslope Deposits

Qc **Holocene and Pleistocene hillslope colluvium (Quaternary)—**Unit Qc consists of locally-derived deposits on moderately steep hillslopes in mountains. Colluvium is very extensive in the mountains, but is mapped only where sufficiently thick and extensive as to obscure underlying bedrock. Deposits are very poorly sorted, ranging from clay to cobbles and boulders. Clasts typically are subangular to angular because they have not been transported very far. Bedding is weak and dips are quite steep, reflecting the steep depositional environment. Deposits are a few meters thick or less; thickest deposits are found at the bases of hillslopes. Some stable hillslopes are covered primarily with Pleistocene deposits, which are typically reddened and enriched in clay. Other more active hillslopes are covered with Holocene deposits, which have minimal soil development.

Bedrock Units

Tpu **Upper Pantano Formation (Oligocene to Miocene)—**A heterolithic assemblage of medium- to thick-bedded sandstone, pebbly sandstone, and pebble-cobble-boulder conglomerate, with intervals of thin- to medium-bedded sandstone and mudstone. Clasts, which range from rounded to sub-angular, consist chiefly of Bisbee Group sandstone and mudstone along with a distinctive coarse-grained, crystal-rich quartz –biotite porphyry. Minor volcanic clasts are also present. The base of the unit in many areas is defined as the top a crystal-rich, coarse-grained andesite lava. In areas where this lava is absent or concealed, abundant clasts of the lava are common near the base of the unit. A sequence of one or two nonwelded felsic tuffs occur near the base in the easterly adjacent Narrows quadrangle, typically within a sequence of mudstone and thin-bedded to laminated sandstone. Also, in the easterly adjacent Narrows quadrangle, a distinctive, limestone boulder-megaclast breccia sheet (Txc) appears to be interbedded with conglomerate near the top of this unit.

Tas **Mafic volcaniclastic sequence (Oligocene)—**Volcaniclastic sandstone and pebbly sandstone mixed with greenish mafic pyroclastic beds. Rocks of this unit are thin- to medium-bedded in the south, but massive to thick-bedded to the north. These rocks directly overlie the porphyritic andesite lava (Ta).

Ta **Porphyritic andesite lava (Oligocene)—**Crystal-rich, coarse-grained andesite lava containing 20-40% plagioclase phenocrysts up to 2 cm. The unit consists of massive, rarely flow-brecciated, amalgamated flows. Along strike to the north, the andesite lava has been dated at 24.9 ± 5.2 Ma (K/Ar plagioclase date with 2s uncertainty [95% confidence interval]), and a sample from the northeastern Rincon Mountains (Mineta Ridge) yielded an age of 26.9 ± 4.8 Ma (2s uncertainty [95% confidence interval]; Shafiqullah et al., 1978).

Tpl **Lower Pantano Formation (Oligocene)—**Medium- to thick-bedded conglomerate, pebbly sandstone, and sandstone, typically reddish colored. Clasts, which range from rounded to sub-angular consist chiefly of crystal-rich, coarse-grained quartz porphyry, and various Bisbee Group sandstone and mudstone lithologies. Towards the northern edge of the basin limestone clasts abruptly appear and are locally abundant. Several percent intermediate composition volcanic clasts are also present, and sparse granitoid clasts.

Tpfl **Limestone and mudstone unit of the lower Davidson Canyon facies, Pantano Formation (Oligocene)—**At the base of the lower Davidson Canyon facies of the Pantano Formation, a sequence of mudstone and thin- to medium-bedded sandstone and pebbly sandstone is present that locally includes abundant thin- to medium-bedded limestone. The limestone varies from quartz sandy pisoid packstone to laminated micrite. Some of the micritic beds are strongly fetid.

Tr **Rhyolite ash-flow tuff (Oligocene)—**Along Interstate 10, several exposures of densely welded, crystal-rich quartz, sanidine, plagioclase, biotite – phyric rhyolite ash-flow tuff are present, directly overlying (with angular unconformity) the Bisbee Group. The tuff also appears to overlap strands of a major east-west striking, north-side-down fault just to the south of Interstate 10. The rhyolite has been dated at 33.01 ± 0.38 Ma (weighted mean of six single-crystal $^{40}Ar/^{39}Ar$ sanidine dates from unpublished report by Lisa Peters, New Mexico Bureau of Mines and Mineral Resources [1999], sample 5-6-98-1; 2s uncertainty). Previously determined dates are as follows: 33.6 ± 5.4 Ma (K-Ar biotite), and 37.6 ± 2.2 Ma (K-Ar sanidine; both by Damon and Bikerman, 1964, given as recalculated by Reynolds et al., 1986), and 34.4 ± 1.6 Ma (K-Ar biotite; Dickinson and Shafiqullah, 1989; 2s uncertainty [95% confidence interval] given for all dates).

Ti **Dacitic lava dome (Oligocene)—**A moderately crystal-rich, plagioclase, biotite-phyric dacitic lava dome occurs along the southern edge of Mount Fagan quadrangle. Marvin et al. (1973) report a K/Ar biotite age of 28.0 ± 1.1 Ma for this rock.

Tq **Quartz porphyry (Tertiary)—**Dikes, plugs and irregular hypabyssal bodies of coarse-grained, crystal-rich quartz porphyry. The porphyry contains quartz phenocrysts up to 4mm along with altered plagioclase phenocrysts up to 5mm. Mafic minerals are typically strongly altered. The unit is commonly argillic altered to advanced argillic altered and hematite stained.

TKm **Fine-grained mafic dikes and intrusive bodies (Tertiary – Cretaceous)—**Dark green finely crystalline mafic dikes typically intrude the upper portion of the Empire Mountains stock (Ke).

Ke **Empire Mountains stock (Upper Cretaceous)—**The upper part of this pluton is a medium-grained granodiorite containing 10-30% biotite and hornblende. Within its core, the pluton is medium-grained to coarse-grained, contains less than 10% mafic minerals, and appears to be slightly more felsic. Marvin et al. (1973) dated the stock at 71.90 $\pm$ 2.50 Ma (K/Ar biotite).

Kgdy **Corona de Tucson stock, younger phase (Upper Cretaceous)—**Granitoid mapped by Finnell (1971) as unit TKm and referred to as a quartz monzonite by Marvin et al. (1973) who dated the rock at 75.5 Ma $\pm$ 2.70 (K/Ar, biotite).

Kgd **Corona de Tucson stock (Upper Cretaceous)—**Granitoid mapped by Finnell (1971) as unit Kg and referred to as a quartz monzonite by Marvin et al. (1973) who dated the rock at 75.3 Ma $\pm$ 2.90 (K/Ar, biotite).

Kr **Rhyolite of Mount Fagan (Upper Cretaceous)—**Crystal-rich, densely welded rhyolite ash-flow tuff containing 20-40% phenocrysts of quartz (2-4 mm), plagioclase (1-3 mm), pottasium feldspar (1-3 mm), and biotite (1-2 mm). The tuff is preserved within a large cauldron encompassing most of the Mount Fagan quadrangle and is associated with a wide variety of lithic megabreccia (abundant clasts greater than 1 meter) and mesobreccia (clasts generally smaller than 1 meter) units. The monolithic megabreccia units in this area are characterized by very large (commonly over 100 m wide) megaclasts. In some areas, these clasts are arranged in tabular bodies that represent intact fragments of stratigraphic sequences of the country rock. Large of areas of these monolithic megabreccia units are void of pyroclastic matrix, but generally, thin irregular dikes and stringers of the pyroclastic matrix can be found invading these outcrops.

Krz **Heterolithic mesobreccia**

Krg **Heterolithic megabreccia**

Krd **Crystal-rich dacite tuff megabreccia**

Kra **Andesite megabreccia**

Krc **Well-rounded conglomerate megabreccia (Fort Crittenden)**

Krq **Quartz sandstone megabreccia (Turney Ranch)**

Krb **Bisbee Group megabreccia (Willow Spring – Apache Canyon – Shellenberger Canyon)**

Krl **Limestone megabreccia**

Kd **Crystal-rich dacite ash-flow tuff (Upper Cretaceous)—**Densely welded dacitic ash-flow tuff containing 25%-40% phenocrysts of plagioclase and biotite. The tuff underlies the rhyolite of Mount Fagan in one locality on the south slope of Mount Fagan, and occurs as lithic clasts within the rhyolite of Mount Fagan.

Kdl **Dacitic lava (Upper Cretaceous)**:

Ka **Andesitic lava (Upper Cretaceous)**:

Kfcv **Heterolithic breccia – conglomerate (Upper Cretaceous)**: A massive, poorly exposed, mostly clast-supported unit consiting of a mixture of rounded to well-rounded quartzite cobbles and boulders with quartz sandy matrix and angular to sub-angular, poorly sorted andesitic detritus.

Kfc **Fort Crittenden Formation (Upper Cretaceous)**: Massive to very thick-bedded and thick-bedded, clast-supported conglomerate and pebbly sandstone. Well-rounded to rounded clasts are dominantly quartz sandstone derived from the Bisbee Group.

Kfcf **Fine-grained facies, Fort Crittenden Formation (Upper Cretaceous)**: A fine-grained facies of the Fort Crittenden Formation consisting dominantly of sandstone, and siltstone with minor pebbly sandstone and conglomerate.

Kq **Turney Ranch Formation, Bisbee Group (Lower Cretaceous)—**Medium- to thick-bedded quartz sandstone interbedded with thin- to medium-bedded, typically reddish colored, silty mudstone and shale. The mudrocks are typically reddish colored. The quartz sandstone is typically cross-stratified in bed-scale bedforms that range from tabular-planar to wedge-planar in shape. The quartz sandstone is generally strongly fractured and locally shattered.

Kb **Willow Spring – Apache Canyon – Shellenberger Canyon lithofacies, Bisbee Group (Lower Cretaceous)—**Thin- to thick-bedded, argillaceous, feldspathic sandstone or arkose and pebbly sandstone interbedded with olive gray, typically pyrite-bearing, shale and mudstone. Pebbly sandstone beds contain abundant black and white, well-rounded to rounded chert clasts. Some intervals include thin- to medium-bedded limestone beds. The thin limestone beds tend to be laminated, and the medium-bedded limestone commonly consists of mollusc shell, skeletal wackstone with dark-colored, micritic, fetid matrix. Bed-scale cross-stratified bedforms dominate the sandstone units, which locally contain Bouma (1962) sequence turbidite sedimentary sequences.

Kbl **Limestone, Willow Spring – Apache Canyon lithofacies, Bisbee Group (Lower Cretaceous)—**Limestone-rich sequences of this lithofacies, found generally near the base of the map unit.

KJg **Glance Conglomerate, Bisbee Group (Lower Cretaceous – Jurassic)—**Conglomerate, coarse-grained arkose, and sparse limestone that is present locally at the base of the Bisbee Group. North of the Empire Mountains, the Glance Conglomerate is relatively thin or absent and, where present, consists mostly of arkose and clast-supported, rounded to sub-rounded cobble-boulder granodiorite-clast conglomerate. At one locality along Interstate 10, near the four corners of the quadrangles, a limestone-clast conglomerate intertongues with granitoid-clast conglomerate and arkose. In the Empire Mountains, the Glance Conglomerate thickens dramatically to the south into massive to very thick-bedded, commonly monolithic or bimodal, cobble-boulder units with sub-rounded to sub-angular clasts. Three varieties of the Glance Conglomerate, identified based on clast composition, were mapped separately where possible.

KJgg **Monolithic granitoid clast Glance Conglomerate**

KJgq **Monolithic quartzite clast Glance Conglomerate**

KJgl **Monolithic limestone clast Glance Conglomerate**

J^{2}g **Gardner Canyon Formation (Jurassic – Triassic)—**A heterolithic assemblage of dark red mudstone or slate, volcaniclastic sandstone, and conglomerate, with sparse volcanic flows. Estimated at up to 350 meters thick by Finnell (1971).

J²gm **Mudstone, Gardner Canyon Formation (Jurassic – Triassic)**—Dark red mudstone, typically strongly cleaved.

J²gd **Crystal-rich dacitic ash-flow tuff, Gardner Canyon Formation (Jurassic – Triassic)**—A single exposure of a 15 meter-thick, crystal-rich, dacitic ash-flow tuff with 2-15% lithic clasts, many of which are red mudstone. Associated with volcaniclastic sandstone and conglomerate.

¼l **Paleozoic limestone, undifferentiated (Devonian – Permian)—**A map unit that encompasses all Paleozoic carbonate units. The unit is employed in areas of poor exposure and/or where carbonate rocks are intensely recrystallized, or where structural complexity makes it difficult to assign more specific unit names.

Prv **Rain Valley Formation (Permian)—**Thin- to medium-bedded, slightly cherty limestone with local thin beds of yellowish-gray to pinkish-gray, fine- to medium-grained quartz sandstone and sandy limestone. Limestone is typically recrystallized, but skeletal packstone and grainstone textures preserved locally. Up to 120 meters thick.

Pc **Concha Limestone (Permian)—**Thick-bedded limestone with abundant chert nodules. Quartz sandy intervals and dolostone present near the base. Limestone is typically recrystallized, but skeletal packstone and grainstone textures preserved locally. Approximately 180 meters thick.

Ps **Sherrer Formation (Permian)—**A tripartite unit consisting mostly of quartz sandstone with a medial carbonate unit.

Psu **upper—**Light-gray to pinkish-gray fine- to medium-grained, calcareous, cross-stratified, quartz sandstone. Up to 45 meters thick.

Psm **middle—**Gray to pale orange, thin- to medium-bedded dolostone and dolomitic limestone. Approximately 35 meters thick.

Psl **lower—**Light yellowish-brown, fine- to medium-grained, calcareous, cross-stratified, quartz sandstone with a few thin beds of dolostone and red marly siltstone at the base. Approximately 100 meters thick.

Pe **Epitaph Formation (Permian)—**A tripartite unit consisting of dolostone, limestone, siltstone and gypsum with a medial member containing gypsum beds and otherwise dominated by siliciclastic rocks.

Peu **upper—**Medium- to thick-bedded gray to dark gray dolostone and limestone, locally containing chert nodules. Approximately 25 meters thick.

Pem **middle—**Yellowish-gray to pale-pink marlstone, siltstone, and silty dolostone, locally with beds of gypsum. Unit is commonly deeply weathered with characteristic float blocks of honeycombed calcareous siltstone. Approximately 250 meters thick.

Pel **lower—**Thin- to medium-bedded dark gray dolostone, locally containing quartz-filled vugs. Approximately 100 meters thick.

Pcl **Colina Limestone (Permian)—**Thick-bedded, medium to dark gray micritic limestone, commonly with abundant millimeter-scale, white calcite veins. Approximately 20 meters thick.

P³e **Earp Formation (Permian - Pennsylvanian)—**Greenish-gray, light brown, and pale-red thin- to medium-bedded, quartz sandstone and quartz sandstone with sparse, thin-bedded limestone, and a thin lenticular bed of chert pebble conglomerate about 100 meters above the base. Approximately 275 meters thick.

³h **Horquilla Limestone (Pennsylvanian)—**Medium- to thick-bedded gray cherty limestone with interbeds of thin- to medium-bedded silty greenish-gray shale and micritic limestone. Limestone is typically recrystallized, but skeletal and pelletal packstone and grainstone textures preserved locally. Up to 300 meters thick.

Mek **Red mudstone (Mississippian)—**A red mudstone marker unit near the top of Escabrosa Limestone that in some areas occurs as cavity-filling units in the upper Escabrosa Limestone. In many areas, this unit appears as a black, fine- to medium-grained hornfels containing sub-angular to angular chert pebbles. The unit probably correlates with the Black Prince Limestone of Finnell (1971). 0 to 15 meters thick.

Me **Escabrosa Limestone (Mississippian)—**Massive to thick-bedded and very thick-bedded cherty recrystallized limestone or coarsely crystalline marble. Skeletal and pelletal packstone and grainstone textures preserved locally. Up to 180 meters thick.

Dm **Martin Formation (Devonian)—**Massive to very thick-bedded, light gray to white, recrystallized, sugary, micritic dolostone. Finnell (1971) reports white quartzite and greenish-gray hornfels and shale units, garnetite and serpentite limestone near contact with the Empire Mountains stock, and a 30cm conglomeratic sandstone at the base. Approximately 60 meters thick.

ºa **Abrigo Formation (Cambrian)—**A mixed siliciclastic and carbonate unit consisting of interbedded thin- to medium-bedded, greenish-gray calcareous siltstone, silty shale and shale and variable quartz sandy limestone and dolostone. In general, the unit contains more carbonate rocks up section. Approximately 250 meters thick.

ºb **Bolsa Quarzite (Cambrian)—**Medium- to thick-bedded, cross-stratified, light pinkish-gray to purplish-red, medium- to coarse-grained quartz sandstone, with feldspathic quartz sandstone and pebbly conglomerate near the base. Thin shale intervals are present in the upper part. Approximately 120 meters thick.

Yg **Granite (Mesoproterozoic)—**Coarse-grained equigranular to k-feldspar-porphyritic granite containing less than 10% biotite.

Xgd **Granodiorite (Paleoproterozoic)—**Medium-grained equigranular granodiorite containing 10-30% mafic minerals, chiefly biotite.

Xp **Pinal Schist (Paleoproterozoic)—**A metapelitic unit including a wide variety of rock types from silvery gray fine-grained chloritic crenulated schist to dark grayish-green, quartz veined biotite schist, and banded, quartz veined biotite schist.

REFERENCES CITED

Anderson, S.R., 1988, Potential for aquifer compaction, land subsidence, and earth fissures in the Tucson basin, Pima County, Arizona: U.S. Geological Survey Hydrologic Investigations Atlas HA-713, 3 sheets, scale 1:250,000.

Anderson, S.R., 1989, Potential for aquifer compaction, land subsidence, and earth fissures in Avra Valley, Pima and Pinal counties, Arizona: U.S. Geological Survey Hydrologic Investigations Atlas HA-718, 3 plates, scale 1:250,000.

Archibald, L.E., 1987, Stratigraphy and sedimentology of the Bisbee Group in the Whetstone Mountains, southeastern Arizona, *in* Dickinson, W.R., and Klute, M.A., eds., Mesozoic rocks of southern Arizona and adjacent areas: Arizona Geological Society Digest, v. 18, p. 273-282.

Arizona Geological Survey, 1988, Earth fissures discovered near CAP canals: Arizona Geology, v. 18, n. 4, p. 10.

Balcer, R.A., 1984, Statigraphy and depositional history of the Pantano Formation (Oligocene-early Miocene), Pima County, Arizona: Tucson, University of Arizona, M.S. thesis, 107 p.

Betancourt, J.L., 1990, Tucson's Santa Cruz River and the arroyo legacy: unpublished Ph.D. dissertation, University of Arizona, 239 p.

Bilodeau, W.L., 1979, Early Cretaceous tectonics and deposition of the Glance Conglomerate, southeastern Arizona: California, Stanford University, Ph.D. dissertation, 145 p.

Bilodeau, W.L., 2001, Laramide contractional reactivation of older Mesozoic extensional faults in the southern Mule Mountains of southeastern Arizona: Geological Society of America, Abstracts with Programs, v. 33, n. 3, p. 38.

Bilodeau, W.L., Kluth, C.F., and Vedder, L.K., 1987, Regional stratigraphic, sedimentologic and tectonic relationships of the Glance Conglomerate in southeastern Arizona, *in* Dickinson, W.R., and Klute, M.A., eds., Mesozoic rocks of southern Arizona and adjacent areas: Arizona Geological Society Digest, v. 18, p. 229-256.

Bouma, A. H., 1962, Sedimentology of some flysch deposits: Elsevier, Amsterdam, 168 pp.

Brennan, D.J., 1957, Geological reconnaissance of Cienega Gap, Pima County, Arizona: Tucson, University of Arizona, Ph.D. dissertation, 53 p.

Bull, W.B., 1991, Geomorphic Response to Climatic Change, New York: Oxford University Press, 326 p.

Bull, W.B., and Pearthree, P.A., 1988, Frequency and size of Quaternary surface ruptures on the Pitaycachi fault, northeastern Sonora, Mexico: Bull. Seis. Soc. Amer., v. 78, p. 956-978.

Damon, P.E., and Bikerman, M., 1964, Potassium-argon dating of post-Laramide plutonic and volcanic rocks within the Basin and Range province of southeastern Arizona and adjacent areas: Arizona Geological Society Digest, v. 7, p. 63-78.

Demsey, K.A., and Pearthree, P.A., 1994, Surficial and environmental geology of the Sierra Vista area, Cochise County, Arizona: AZGS OFR 94-6, 14 p., scale 1:24,000.

Demsey, K.A., House, P.K., and Pearthree, P.A., 1993, Detailed surficial geologic map of the southern piedmont of the Tortolita Mountains, Pima County, southern Arizona: Arizona Geological Survey Open-File Report 93-14, 8 p. scale 1:24,000.

Dickinson, W.R., and Shafiqullah, Muhammad, 1989, K-Ar and F-T ages for syntectonic mid-Tertiary volcanosedimentary sequences associated with the Catalina core complex and San Pedro trough in southern Arizona: Isochron/West, n. 52, p. 15-27.

Dickinson, W.R., Klute, M.A., and Bilodeau, W.L., 1987, Tectonic setting and sedimentologic features of Upper Mesozoic strata in southeastern Arizona, *in* Davis, G.H., and VandenDolder, E.M., eds., Geologic diversity of Arizona and its margins: Excursions to choice areas: Arizona Geological Survey Special Paper 5, p. 266-279.

Dobyns, H.R., 1981, From fire to flood, Historic human destruction of Sonoran desert riverine oases, Socorro, NM., Ballena Press, 222 p.

Drewes, H.D., 1977, Geologic map and sections of the Rincon Valley quadrangle, Pima County, Arizona: U.S. Geological Survey Miscellaneous Investigations Series Map I-997, 1 sheet, scale 1:48,000.

DuBois, S.M., Smith, A.W., Nye, N.K., and Nowak, T.A., 1982, Arizona Earthquakes, 1776-1980: Arizona Bureau of Geology and Mineral Technology Bulletin 193, 456 p., scale 1:1,000,000.

Finnell, T.L., 1970, Formations of the Bisbee Group, Empire Mountains quadrangle, Pima County, Arizona, in Changes in stratigraphic nomenclature by the U.S. Geological Survey, 1968: U.S. Geological Survey Bulletin 1294-A, p. A28-A35.

Finnell, T.L., 1971, Preliminary geologic map of the Empire Mountains quadrangle, Pima County, Arizona: U.S. Geological Survey Open-File Report 71-0106, 2 sheets, scale 1:48,000.

Galloway, Devin, Jones, David R., and Ingerbritsen, S.E., 1999, Land subsidence in the United States: US Geological Survey Circular 1182, 177 p.

Gile, L.H., Hawley, J.W., and Grossman, R.B., 1981, Soils and geomorphology in the basin and range area of southern New Mexico -- guidebook of the Desert Project: New Mexico Bureau of Mines and Mineral Resources Memoir 39, 222 p.

Hardy, J. J., 1997, Superimposed Laramide and middle Tertiary deformations in the northern Santa Rita Mountains, Pima County, Arizona, Golden, Colorado School of Mines: unpublished Ph.D. dissertation, 185 pp, 1 plate, scale 1:12,000.

Hatch, M.A., 1991, Global positioning system measurement of subsidence in the Tucson Basin, Pima County, Arizona: Tucson, University of Arizona, M.S. thesis, 87 p.

Helmick, Walter, R., 1986, The Santa Cruz River terraces near Tubac, Santa Cruz County, Arizona; Tucson University of Arizona, M.S. thesis, 96 p.

Jackson, G.W., 1989, Surficial geologic maps of the northeastern, southeastern, and southwestern portions of the Tucson metropolitan area: Arizona Geological Survey Open-File Report 89-2, 6 p., 7 sheets, scale 1:24,000.

Jackson, G.W., 1990, Quaternary geologic map of the Corona de Tucson 7.5' quadrangle, Arizona: Arizona Geological Survey Open-File Report 90-3, 6 p., scale 1:24,000.

Johnson, R.A., and Loy, K.L., 1992, Seismic reflection evidence of seismogenic low-angle faulting in southeastern Arizona: Geology, v. 20, n. 7, p. 597-600.

Katzer, Keith, and Schuster, J.H., 1984, The Quaternary geology of the the northern Tucson basin, Arizona and its archaeological implications: Tucson, University of Arizona Dept. of Geosciences, M.S. prepublication manuscript.

Keith, S.B., Gest, D.E., DeWitt, Ed, Woode Toll, Netta, and Everson, B.A., 1983, Metallic mineral districts and production in Arizona: Arizona Bureau of Geology and Mineral Technology Bulletin 194, 58 p., 1 sheet, scale 1:1,000,000.

Klawon, J.E., Dickinson, W.R., and Pearthree, P.A., 1999, Surficial geology and geologic hazards of the northern Tucson basin, Tucson North and Sabino Canyon 7 ½' quadrangles: Arizona Geological Survey Open-File Report 99-21, 21 p. 1 sheet, scale 1:24,000.

Klute, M.A., 1991, Sedimentology, sandstone petrofacies, and tectonic setting of the late Mesozoic Bisbee basin, southeastern Arizona: Tucson, University of Arizona Ph.D. dissertation, 268 p.

Machette, M.N., 1985, Calcic soils of the southwestern United States: in Weide, D.L., ed., Soils and Quaternary Geology of the Southwestern United States: Geological Society of America Special Paper 203, p. 1-21.

Marvin, R.F., Stern, T.W., Creasey, S.C., and Mehnert, M.H., 1973, Radiometric ages of igneous rocks from Pima, Santa Cruz, and Cochise Counties, southeastern Arizona: U.S. Geological Survey Bulletin 1379, 27 p.

McKittrick, M.A., 1988, Surficial geologic maps of the Tucson metropolitan area: Arizona Geological Survey Open-File Report 88-18, 7 p., 12 sheets, scale 1:24,000.
Menges, C.M., and McFadden, L.D., 1981, Evidence for a latest Miocene to Pliocene transition from Basin-Range tectonic to post-tectonic landscape evolution in southeastern Arizona: Arizona Geological Society Digest 13, p. 151-160.
Menges, C.M., and Pearthree, P.A., 1989, Late Cenozoic tectonism and landscape evolution in Arizona, in Jenney, J., and Reynolds, S.J., eds., Geologic Evolution of Arizona: Arizona Geological Society Digest 17, p. 649-680.
Myrick, David F., 1975, Railroads of Arizona Vol. 1; the southern roads, Berkeley, California, Howell-North Books.
Parker, J.T.C., 1995, Channel change on the Santa Cruz River, Pima County, Arizona: U.S. Geological Survey Water-Supply Paper 2429, 58 p.
Pearthree, P.A., 1986, Late Quaternary faulting and seismic hazard in southeastern Arizona: Arizona Geological Survey Open-File Report 86-8, 22 p.
Pearthree, P.A., 1998, Quaternary fault data and map for Arizona: Arizona Geological Survey Open-File Report 98-24, 122 p., map scale 1:750,000.
Pearthree, P.A., and Biggs, T.H., 1999, Surficial geology and geologic hazards of the Tucson Mountains, Pima County, Arizona: Arizona Geological Survey Open-File Report 99-22, 12 p., 2 sheets, scale 1:24,000.
Pearthree, P.A., and Calvo, S.S., 1987, The Santa Rita fault zone: Evidence for large magnitude earthquakes with very long recurrence intervals, Basin and Range province of southeastern Arizona: Bull. Seis. Soc. Amer., v. 77, p. 97-116.
Pearthree, P.A., and Youberg, A., 2000, Surficial geology and geologic hazards of the Green Valley-Sahuarita Area, Pima County, Arizona: Arizona Geological Survey Open-File Report 99-22, 12 p., 2 sheets, scale 1:24,000.
Pearthree, P.A., Demsey, K.A., Onken, Jill, Vincent, K.R., and House, P.K., 1992, Geomorphic assessment of flood-prone areas on the southern piedmont of the Tortolita Mounstins, Pima County, Arizona: Arizona Geological Survey Open-File Report 91-11, 31 p., scale 1:12,000 and 1:24,000, 4 sheets.
Peizhen, Z., Molnar, P., and Downs, W.R., 2000, Increased sedimentation rates and grain sizes 2-4 Myr ago due to the influence of climate change on erosion rates: Nature, v. 410, p. 891-897.
Percious, J.K., 1968, Geology and geochronology of the Del Bac Hills, Pima County, Ariozna, *in* Titley, S.R., ed., Southern Arizona Guidebook III: Arizona Geological Society, p. 199-207.
Platt, W.S., 1963, land-surface subsidence in the Tucson area: University of Arizona unpublished Masters Thesis, Department of Geology, 38 p.
Pope, G.L., Rigas, P.D., and Smith, C.F., 1998, Statistical summaries of streamflow data and characteristics of drainage basins for selected streamflow-gaging stations in Arizona through Water Year 1996: U.S. Geological Survey Water-Resources Investigations Report 98-4225, 907 p.
Ransome, F.L., 1919, The copper deposits of Ray and Miami: U.S. Geological Survey Professional Paper 115, 192 p., map-scale 1:125,000.
Reynolds, S.J., Florence, F. P., Welty, J. W., Roddy, M. S., Currier, D. A., Anderson, A. V., and Keith, S. B., 1986, Compilation of radiometric age determinations in Arizona: Tucson, Arizona Bureau of Geology and Mineral Technology Bulletin 197, 258 p.
Richard, S.M., Spencer, J.E., Ferguson, C.A., and Youberg, A., Layton, D. W., and Finnell, T. L., 2001, Geologic map of the Vail 7 ½' Quadrangle, eastern Pima County, Arizona: Arizona Geological Survey Digital Geologic Map 12, scale 1:24,000 (1 sheet), with 33 page text.

Schumann, H.H., 1992, Land subsidence and earth-fissure hazards near Luke Air Force Base, Arizona, *in* U.S. Geological Survey Subsidence Interest Group conference, Edwards Air Force Base, Antelope Valley, California, November 18-19, 1992 - Abstracts and Summary: US Geological Survey Open-File Report 94-532, p. 18-21.Sellers, W.D., and Hill, R.H., 1974, Arizona Climate, 1931-1972: Tucson, University of Arizona Press, 616 p.

Scott, R. W., 1987, The bivalve, Musculiopsis MacNeill, in Lower Cretaceous non-marine strata, Rocky Mountains: Contributions to Geology, University of Wyoming, v. 25, p. 29-33.

Sellers, W.D., and Hill, R.H., 1974, Arizona Climate, 1931-1972: Tucson, University of Arizona Press, 616 p.

Shafiquallah, M., Damon, P.E., Lynch, D.J., Reynolds, S.J., Rehrig, W.A., and Raymond, R.H., 1980, K-Ar geochronology and geologic history of southwestern Arizona and adjacent areas: Arizona Geological Society Digest, v. 12, p. 201-260.

Shafiqullah, M., Damon, P.E., Lynch, D.J., Kuck, P.H., and Rehrig, W.A., 1978, Mid-Tertiary magmatism in southeastern Arizona, *in* Callender, J.F., Wilt, J.C., Clemons, R.E., and James, H.L., eds., Land of Cochise, southeastern Arizona: New Mexico Geological Society 29th Field Conference Guidebook, p. 231-241.

Skotnicki, S.J., 2001, Geologic map of the Mescal 7 ½' Quadrangle, Pima and Cochise Counties, Arizona: Arizona Geological Survey Digital Geologic Map 09, scale 1:24,000 (1 sheet), with 17 page text.

Slaff, Steve, 1993, Land subsidence and earth fissures in Arizona, Arizona Geological Survey Down-to-Earth Series 3, 24 p.

Spencer, J.E., Ferguson, C.A., Richard, S.M., Orr, T.R., and Pearthree, P.A., Gilbert, W. G., and Krantz, R. W., 2001, Geologic map of The Narrows 7 ½' Quadrangle and the southern part of the Rincon Peak 7 ½' Quadrangle, eastern Pima County, Arizona: Arizona Geological Survey Digital Geologic Map 10, scale 1:24,000 (1 sheet), with 32 page text.

Tyrell, W. W., Jr., 1957, Geology of the Whetstone Mountain area, Cochise and Pima Counties, Arizona, New Haven, Connecticut, Yale University: unpublished Ph.D. disseratation.

Tyrell, W. W., Jr., 1965, Geology of the Whetstone Mountain area, Cochise and Pima Counties, Arizona (abs.): Dissertation abstracts., v. 25, no. 6, p. 3516.

U.S. Geological Survey, 2001, Real-time data for selected stream gaging sites in Arizona website; annual peak flow data.

Western Regional Climate Center, 2001, Arizona climate summaries, in Western U.S. historical climate summaries, WRCC Web Page, Desert Research Institute, University of Nevada.

Wood, M.L., House, P.K., and Pearthree, P.A., 1999, Historical geomorphology and hydrology of the Santa Cruz River: Arizona Geological Survey Open-File Report 99-13, 98 p., 1 sheet, scale 1:100,000.

Yen, T, 1951, Fresh-water mollusks of Cretaceous age from Montana and Wyoming: U. S. Geological Survey Professional Paper 233-A, 20 pp.